# The magnetic polarity time scale across the Permian–Triassic boundary

MAUREEN B. STEINER

*Department of Geology/Geophysics, University of Wyoming, Laramie, Wyoming 82071, USA (e-mail: magnetic@uwyo.edu)*

**Abstract:** Early Triassic and Late to Middle Permian magnetostratigraphic investigations are numerous and span the globe. More than 20 magnetostratigraphic sequences have documented all or part of the Early Triassic geomagnetic field polarity, and > 27 have examined the Late and Middle Permian; 13 span the Permian–Triassic boundary. In order to assess the exact polarity sequence in the time period surrounding the Permian–Triassic boundary, the sequences have been compared diagrammatically. Four distinctive intervals of geomagnetic polarity characterize the Early Triassic, and have been named for discussion purposes: Gries N, Diener R-N, Smith N, and Spath N. A polarity pattern for the Mid- and Late Permian is also recognizable. The Mid- and Late Permian are characterized by two normal polarity intervals (Chang N and Capitan N) of greater apparent duration than those of the Early Triassic. Below the Permo-Triassic Gries N, a distinctive short duration reversed-normal-reversed polarity pattern characterizes the uppermost Changhsingian. The oldest normal polarity in the Middle Permian occurred during the Wordian Stage, established by results from three global sequences. Therefore, the geomagnetic field resumed reversing behaviour after the ~50 Ma-long constant polarity of the Kiaman Reversed Polarity Superchron ('Illawarra reversals') during the Mid- to Late Wordian, or ~267 Ma.

Very significantly, the magnetostratigraphic summary from this work indicates that the Siberian Traps were active in the Late Permian and spanned the Permian–Triassic boundary. This new geomagnetic polarity dating of the massive Siberian flood basalt activity suggests long-term eruption and environmental degradation, therefore making this igneous activity the most likely cause of the end-Permian mass extinctions. Magnetostratigraphy suggests that eruptions probably commenced in the Late Guadalupian; therefore, the eruptions of two large igneous provinces, Emishan and Siberian, were probably partly simultaneous during part of the Mid- to Late Permian. Environmental havoc throughout the late Mid- and Late Permian is easy to imagine, stressing the environment prior to probably more voluminous eruptions at the end of the Guadalupian and Permian. Siberian eruptions continued through the early Early Triassic, and probably contributed to the slow biotic recovery.

The greatest demise of life forms on this planet occurred at the close of the Permian Period. The quest to understand the cause of this largest of mass extinctions would be aided by the knowledge of the exact sequence of geomagnetic field polarity reversals around that time, because, when preserved, the magnetic polarity sequence is a constant, independent of facies, climatic zonation, endemism, and other variables that have hampered global Permian–Triassic biostratigraphical correlation.

The most accurate assessment of the geomagnetic field polarity changes during the Late Permian, the Early Triassic, and their mutual boundary will be one determined from examination of all data sources, that is, marine and terrestrial sedimentary strata and igneous rocks (Siberian Traps, Emishan Basalts). Despite the fact that marine sequences allow better age control because of their faunal content, terrestrial and igneous sequences commonly record the geomagnetic field more faithfully because of their greater magnetic mineral content and less chemically reactive depositional setting.

This investigation, therefore, has compiled nearly all of the global magnetostratigraphic results of this time interval. The compilation was restricted to data, excluded publications that consisted solely of summaries, but has included two sets of unpublished data because of their importance in assessing the magnetostratigraphy of the Middle Permian. Some published data have not been included because of the difficulty of including the many results that presently exist into a single clearly readable diagram. Because of this, older studies in which stratal age control was poorly known beyond the period assignment (e.g. Valencio *et al.* 1977) are not included in the diagrams. Furthermore, studies published in regional journals not readily accessible in North

*From:* LUCAS, S. G., CASSINIS, G. & SCHNEIDER, J. W. (eds) 2006. *Non-Marine Permian Biostratigraphy and Biochronology*. Geological Society, London, Special Publications, **265**, 15–38.
0305-8719/06/$15.00 

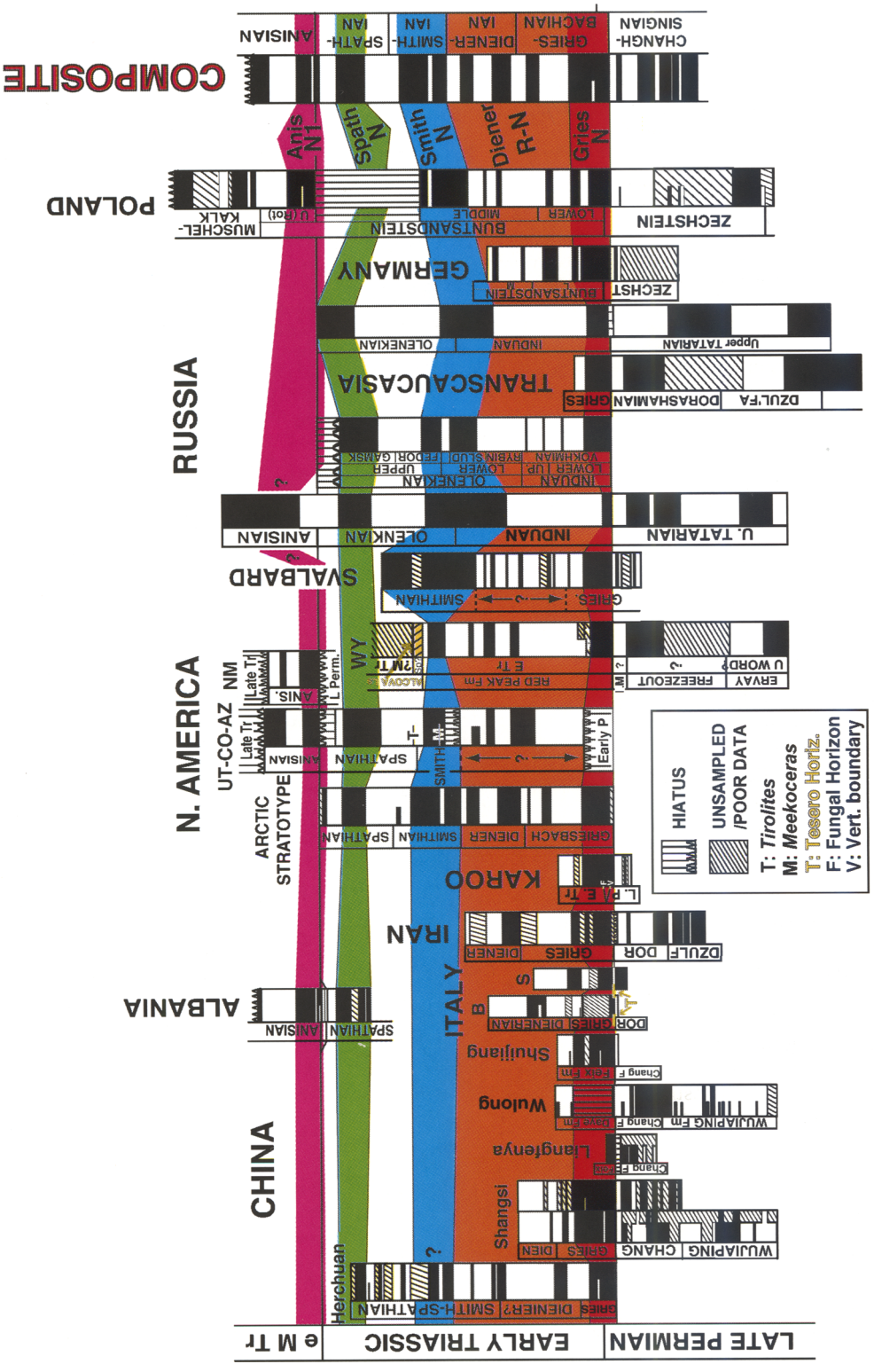

American libraries (and possibly not referenced in North American databases) may have been unintentionally excluded from this compilation.

The compilation is displayed as two diagrams. Results from the Early Triassic are displayed in Figure 1, and those from the Mid- and Late Permian in Figure 2. The Early Triassic is examined first in this assessment of the Permian–Triassic geomagnetic polarity sequence, because a common polarity pattern is apparent in most Early Triassic sequences and easily correlated among them, in sharp contrast to that of the preceding Mid- and Late Permian time interval.

## The Early Triassic

The Early Triassic polarity pattern is generally readily recognizable among global sequences. All or part of the Early Triassic magnetic polarity sequence has been investigated in at least 19 locations globally. Of these magnetostratigraphic sequences, six span approximately the entire Early Triassic; and 13 span the boundary between the Permian and Triassic.

Numerical ages are not used in Figure 1, because no radiometric ages have been determined for the Early Triassic except that of the Permian–Triassic boundary. Lacking Early Triassic numerical ages, various scaling methods have been applied (e.g. Sweet & Bergstroem 1986; Ogg, in Gradstein *et al.* 2004, chapter 17). Ogg assigned Early Triassic radiometric ages based on extrapolation between the Permian–Triassic boundary age and U–Pb-dated tuffs at the Mid- Triassic Anisian–Ladinian boundary, and employed assumptions about the length of the Early Triassic and the length of ammonite zones. However, the Anisian–Ladinian U–Pb dates are not entirely in agreement, varying by $\pm 1.0$ Ma, and have error limits of ~0.5 to 1 Ma. Because these numerical ages assigned to the Early Triassic by Ogg have not been verified by geochronological studies, that numerical time scale is employed in Figure 1.

Individual magnetostratigraphic sequences were plotted in the figures by stretching or compressing each entire polarity sequence to approximately fit the master biostratigraphical scale of the figure. No allowances were made for changes in sedimentation rate within a measured section; these changes become evident when the magnetostratigraphies are compared. Sections without biostratigraphical control were simply scaled to the best match of their displayed polarity patterns to those with biostratigraphical constraints.

Early Triassic magnetostratigraphic sequences agree quite well (Fig. 1) and display no polarity-biostratigraphy conflicts. This agreement, in such marked contrast to the Mid- and Late Permian or the Late Triassic, is probably due to relatively accurate recording of the geomagnetic field polarity by most Early Triassic sequences. The Early Triassic geomagnetic field polarity behaviour appears to be no different in reversal frequency than that of, for example, the Late Triassic. The most likely reason for the great similarity among Early Triassic records of magnetic stratigraphy is the fact that most of the Early Triassic sequences have significant terrestrial sedimentary contributions: Early Triassic strata are either terrestrial deposits, marginal marine deposits, or represent marine depositional environments that received significant terrestrial detritus. Detrital terrestrial sediment provides far more magnetic mineral grain carriers (magnetite, hematite, etc) than are commonly available in wholly marine settings.

A second factor is the fact that $Fe^{2+}$ ions are readily mobile in solutions that have reducing pH values. Magnetite ($Fe_3O_4$) is dominantly composed of $Fe^{2+}$ ions; hematite ($Fe_2O_3$) also contains a portion of $Fe^{2+}$ ions, as do iron sulphides. The biogenic activity in shallow marine environments creates a reducing pH. Therefore, under common marine sedimentary rates of deposition, magnetic grains deposited in the shallow marine environment are readily dissolved; hence the magnetic recorders and their information are removed from the (magneto) stratigraphical record. However, the added magnetic mineral input from the influence of greater terrestrial detritus could compensate for the process of dissolution of magnetic mineral grains; that is, the Earth's field

**Fig. 1.** Global magnetostratigraphic correlation of the Early Triassic. Normal (reversed) polarity is black (white); diagonal lines represent unsampled section or poor data. Magnetostratigraphic sequences shown were taken from: **1.** Steiner *et al.* 1989; **2a.** Steiner *et al.* 1989; **2b.** Heller *et al.* 1988; **3.** Steiner *et al.* 1989; **4. & 5.** Heller *et al.* 1995; **6.** (Albania) Muttoni *et al.* 1996, revised Spathian-Anisian boundary from Bachman & Kozur 2004; **7a-b.** Bella and Siusi, Scholger *et al.* 2000; **8.** Besse *et al.* 1998 and Gallet *et al.* 2000; **9.** Ward *et al.* 2005, Steiner *et al.* 2003; **10.** Ogg & Steiner 1991; **11.** Steiner *et al.* 1993; **12.** Molina-Garza *et al.* 1991; Steiner & Lucas 1992; **13.** Steiner *et al.* 1993; unpub. data; **14.** Hounslow *et al.* 1996; **15.** Khramov 1987; **16.** Lozovsky & Molostovsky 1993; **17.** Kotylar *et al.* 1984; **18.** Gurevich & Stautsitay 1985; **19.** Szurlies *et al.* 2003; **20.** Nawrocki 1997.

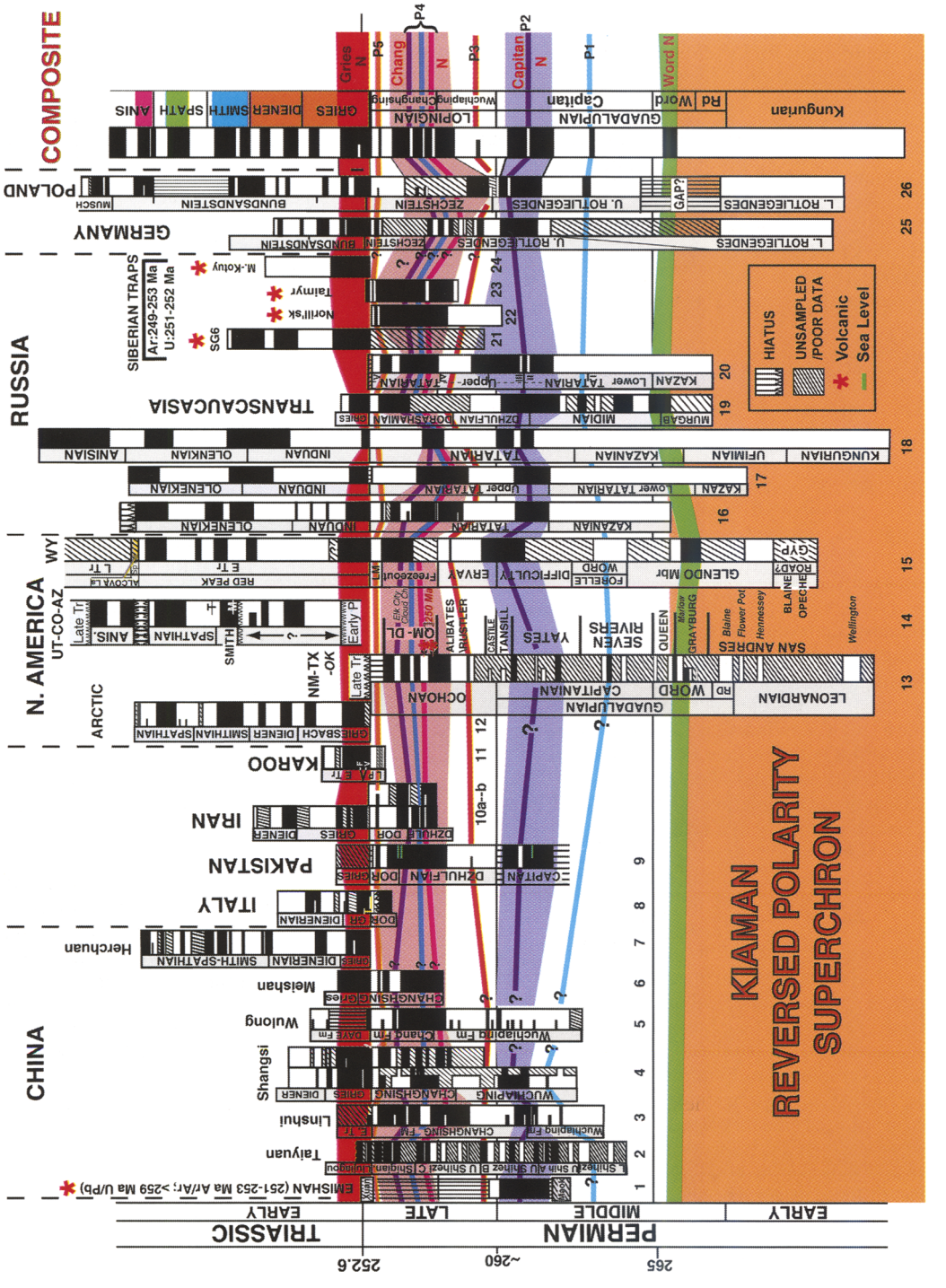

record of the time survives because the greater input of magnetic grains ensures that not all carrier grains are dissolved.

This greater amount of terrestrial sediment input in the Early Triassic may be an effect of the preceding mass extinction; the extinction of life forms, particularly floral, may have allowed greater erosion of the land areas. Because the terrestrial records are the most reliable magnetic data, the terrestrial sequences are described first in the following discussions and followed by the marine records.

### *North America*

Two sequences of largely red-bed sedimentary strata, but with marine strata interfingering, have been studied; both the Moenkopi Formation and the Chugwater Group span most or all of the Early Triassic. In addition two deep-water, nearshore sedimentary sequences of Arctic North America of the Triassic have been investigated, including the global Early Triassic stratotype.

Despite the fact that deposition in the Moenkopi Basin was largely terrestrial red beds, marine incursions into the western part of the basin provide marine faunal control to the red-bed magnetostratigraphy (see Fig. 1, column 11). Ammonite faunas of Smithian (*Meekoceras*) and Spathian (*Tirolites*) ages are present in the western Moenkopi (McKee 1954; Poborski 1954); these are indicated by the letters 'M' and 'T' in Figure 1. Strata overlying the Spathian Moqui Member contain a vertebrate fauna that demonstrates that the Moenkopi Formation (Fig. 1, column 11) continues into the early Anisian Stage of the Middle Triassic (Lucas Morales 1985; Morales 1987). Magnetostratigraphy has been measured in numerous (16) sections across the entire Moenkopi depositional basin (some published – see Steiner *et al.* 1993– and some collected into an archive and obtainable from Steiner). The combined litho- and magnetostratigraphic information has permitted basin-wide correlation of facies and polarity zones.

Column 11 of Figure 1 is a composite of all the Moenkopi studies. Basin-filling began in the eastern part, and the section adjacent to the Uncompahgre uplift, the eastern border of the basin (Helsley & Steiner 1974) spans the entire time of basin-filling, whereas the western part of the basin was filled only in the later half of the Early Triassic and the early Mid-Triassic. Two hiatuses within the Moenkopi deposition were revealed by the magnetostratigraphy. Erosion removed most of the Smithian deposits in the western part of the basin, leaving a conglomeratic facies containing *Meekoceras* ammonites in the clasts; these deposits form the lowest Moenkopi deposits in the western basin, lying directly on Early Permian (Kaibab) limestones. Comparison with the Arctic stratotype sequence (Ogg & Steiner 1991; Fig. 1, column 10) suggests that part of Smithian time is missing in the Moenkopi Formation, even in the westernmost marine deposits (e.g. Shoemaker's Virgin River section; see Steiner *et al.* 1993). The magnetostratigraphy of the eastern basin sections reveals that Moenkopi deposition did not begin at the beginning of the Griesbachian, but slightly later in the Early Triassic, so that the lower part of the Griesbachian Substage (normal polarity) is not represented in the Moenkopi Formation. The second hiatus revealed by magnetostratigraphy is late in Moenkopi deposition, in the latest Spathian, up to and/or including the earliest Anisian. Strata of this time interval were removed across the entire basin. Magnetostratigraphic correlations at this horizon in the western part of the basin display a progressive lateral thinning and, in places, a complete removal by erosion of a relatively short-duration reversed-polarity interval (Grey Mountain magnetozone of Purucker *et al.* 1980) beneath the Anisian vertebrate-bearing strata (Purucker *et al.* 1980; Steiner *et al.* 1993). Again, comparison with the Arctic stratotype sequence suggests that only a short amount of time is missing.

Further north in North America, another red-bed depositional basin also recorded the geomagnetic field polarity during the Early Triassic. The Chugwater Group of western Wyoming contains the marine Griesbachian Dinwoody

**Fig. 2.** Global magnetostratigraphic correlation of the Late and Middle Permian. Normal (reversed) polarity is black (white); diagonal lines represent unsampled section or poor data. Magnetostratigraphic sequences are from: **1.** Huang & Opdyke 1998 (Xuan, Xuanwei Fm; Maok, Makou Fm); **2.** Embleton *et al.* 1996; **3.** Heller *et al.* 1995; **4.** Steiner *et al.* 1989, Heller *et al.* 1988; **5.** Heller *et al.* 1995; **6.** Zhu & Liu 1999, Ziu *et al.* 1999; **7.** Steiner *et al.* 1989; **8.** modified from Scholger *et al.* 2000; **9.** Haag & Heller 1991; **10a.** Besse *et al.* 1998; **10b.** Gallet *et al.* 2000; **11.** Ward *et al.* 2005, Steiner *et al.* 2003; **12.** Ogg & Steiner 1991; **13.** Steiner 2001*a* & *b*; unpub. data; **14.** unpub. data; Steiner *et al.* 1993; **15.** Steiner *et al.* 1993; **16.** Molostovsky 1983, fig. 20 and Lozovsky & Molostovsky 1993; **17.** Gurevich & Slautsitay 1985; **18.** Khramov 1987; **19.** Kotylar *et al.* 1984; **20.** Gialanella *et al.* 1997; **21.** estphal *et al.* 1998; **22.** Fedorenko & Czamanske 1997; **23.** Lind *et al.* 1994; **24.** Gurevich *et al.* 1995; **25.** Menning 1988 and Szurlies *et al.* 2003; **26.** Nawrocki 1997.

Formation shales and limestones, overlain by the red beds of the Red Peak Formation, in turn overlain by the probably marine Alcova Limestone. The marine Dinwoody Formation contains Griesbachian conodonts (Paull & Paull 1986); the Alcova Limestone is thought to be Spathian (Picard *et al.* 1969; Carr & Paul 1983; Storrs 1991), although no diagnostic biostratigraphic proof exists. The Alcova Limestone is overlain by the probably Middle Triassic Crow Mountain or Jelm formations (High & Picard 1967; Lucas 1994). The Red Peak Formation has been studied in a number of sections in western Wyoming; a summary of the magnetostratigraphic results (Steiner *et al.* 1993) is shown as column 13 in Figure 1. The western Wyoming magnetostratigraphy agrees well with the Moenkopi Formation results from further south, as well as with other sections globally. The common polarity pattern recorded in the Red Peak Formation and the lower Moenkopi Formation indicates a common depositional time frame and an essentially accurate recording of the Early Triassic geomagnetic field.

The grey shales and limestones of the Griesbachian Dinwoody Formation were sampled below the Red Peak Formation in the southern Wind River Mountains of western Wyoming, but gave only a Cretaceous normal polarity magnetization (Steiner, unpub. data); this magnetization probably reflects remagnetization associated with the Cretaceous uplift of the Wind River Range during the Laramide orogeny. However, in south-central Wyoming, the lowest ~6 m of the red beds of the Red Peak Formation overlying the Permian Goose Egg Formation were sampled and these recorded normal polarity. The match between the magnetostratigraphies of the western Wyoming Red Peak Formation and the Moenkopi Formation (Steiner *et al.* 1993), combined with the presence of a normal polarity interval in the basal Red Peak beds of southeastern Wyoming, strongly suggests that the lowest Red Peak red beds in southeastern Wyoming are probably lateral equivalents of the Dinwoody Formation. Their normal polarity, therefore, is a representation of the normal polarity interval observed globally in the lower Griesbachian.

The Arctic portion of North America contains the Early Triassic stratotype sequence (Tozer 1967). The strata are marine, and their sequence stratigraphy demonstrates a number of highstands and lowstands of sea level (Ogg & Steiner 1991). Therefore, the relative thicknesses of the polarity intervals are biased by sea-level changes and, to compensate, Ogg (pers. comm. 2004) revised the stratotype polarity sequence in order to minimize the thickness changes related to sea-level changes (Ogg in Gradstein *et al.* 2004, chapter 17). The revised polarity sequence is that displayed in column 10 of Figure 1.

Although Svalbard is no longer part of North America, it was laterally adjacent in Early Triassic time to the Early Triassic stratotype-bearing Canadian Arctic portion of North America. The Svalbard Early Triassic strata were studied (Hounslow *et al.* 1996), and a polarity interpretation was published, but without any supporting palaeomagnetic data on which to base the polarity interpretation. More recently, this same polarity interpretation was used in a sedimentological study (Mork *et al.* 1999), but again without any supporting palaeomagnetic behavioural data. The Svalbard polarity sequence (Fig. 1, column 14) is generally similar to the magnetostratigraphics of the Arctic stratotype and the red-bed sequences of North America; however, numerous additional tiny normal polarity intervals were interpreted in the lower part of the Svalbard record that are not seen in any other sequence, and the lack of published magnetic behavioural data makes it impossible to assess the reality of this large number of short normal polarity intervals.

### *Europe – non-marine*

The terrestrial magnetostratigraphy studied in Europe is that of the Buntsandstein Formation of the Central European Basin (CEB), studied in both Poland and Germany. The Buntsandstein Formation consists of a sequence of red beds that has been divided into three parts ('lower', 'middle', and 'upper') that lie between the Mid-Triassic Muschelkalk and the Permian Zechstein beds. The entire thickness of the Buntsandstein beds has been studied in Poland (Nawrocki 1997), using a combination of outcrop and core samples.

Magnetostratigraphic investigation was subsequently continued through the overlying Middle Triassic Muschelkalk Formation (Nawrocki & Szulc 2000). The polarity sequence Nawrocki (1997) obtained from the Buntsandstein strata is somewhat similar to that of other Early Triassic magnetostratigraphic sequences (Fig. 1, column 20), but appears to lack some polarity intervals. The upper division of the Buntsandstein, the Röt Formation, constitutes a lithological change from terrestrial red beds to hypersaline and marine deposition. Its age is Early Anisian, the faunal basis of which was reviewed in detail by Bachman & Kozur (2004). Bachman & Kozur (2004) also pointed out that

Nawrocki & Szulc's (2000) magnetostratigraphic correlation of the Upper Buntsandstein Röt beds cannot be correct in view of their biostratigraphy. The lithological change represented by the Röt strata probably constitute a sequence-stratigraphic boundary; therefore, the Mid- to Upper Buntsandstein boundary is suggested to represent a hiatus, so that Spathian age strata are absent in the Polish Buntsandstein sequence. The Buntsandstein polarity sequence matches well to that of other global Early and early Mid-Triassic sections if Spathian strata are truly absent (Fig. 2).

In Germany, the 'lower' and the lower portion of the 'middle' Buntsandstein strata have been studied magnetostratigraphically (Szurlies *et al.* 2003; Szurlies 2004; Fig. 1, column 19). The German Buntsandstein polarity results are similar to those of the Polish lower and lower middle Buntsandstein and to the global results.

### *Russia and Transcaucasia*

A very large number of terrestrial red-bed strata have been studied in Russia. Khramov (1987) summarized the results of his abundant investigations, and this summary is shown as column 15 of Figure 1. Molostovsky (1983) also extensively studied the Russian Early Triassic terrestrial strata; the summary presented by Lozovsky & Molostovsky (1993) is shown in column 16 of Figure 1. A clastic sequence transitioning from marine to non-marine deposition in Transcaucasia straddles the Permian–Triassic boundary; the sequence was studied by Kotylar *et al.* (1984) and is shown as column 17 in Figure 1. (The exact same magnetostratigraphy, with the minor exception of moving the basal Griesbachian normal interval down into the Dorashamian, was also published by Zakharov & Sokarev in 1991, but without any supporting palaeomagnetic data from which the magnetostratigraphy was derived.) Gurevich & Slautsitays (1985) studied the marine to non-marine transitional sequence of Upper Permian and Lower Triassic strata on Nova Zemlya (See Fig. 1, column 18). These sections all show the same general pattern, but it had been the practice of Russian authors to eliminate fine-scale details in their magnetostratigraphic summaries. Thus, summary Russian and Transcausian magnetostratigraphies have commonly shown less polarity structure than other sections globally. However, if individual section results are examined (e.g. Molostovsky 1983), the presence of the same short-polarity intervals observed elsewhere is commonly observed.

### *Eurasia – marine*

The Tethys Early Triassic Griesbachian and Dienerian strata have been investigated in Iran (Besse *et al.* 1998; Gallet *et al.* 2000) and in Italy (Scholger *et al.* 2000). In addition, a continuous sequence of the upper part of the Spathian and basal Anisian was studied in Albania (Muttoni *et al.* 1996).

Early Triassic strata were studied in Iran at the Abadeh section (Gallet *et al.* 2000). The Griesbachian and Dienerian Substages were identified by the conodont fauna, which was accompanied by a sparse ammonite fauna. The Griesbachian is characterized by normal polarity succeeded by reversed polarity (Fig. 1, column 8), as is observed globally. The Dienerian begins with normal polarity and is succeeded by a reversed interval. When the gaps in sampling are taken into account (highlighted as diagonal lines in column 8 of Fig. 1), the Griesbachian and Dienerian Substages of the Iranian section agree well with the Arctic stratotype section.

In Italy, two sections were sampled 8 km apart (Scholger *et al.* 2000). The Bulla section is a roadcut, and the Siusi section is a river-cut exposure. Each section contained sampling gaps, and Scholger *et al.* (2000) combined the magnetostratigraphic results from the two into a single polarity column based on the intervals of common polarity and lithostratigraphy. The overall polarity pattern of the Griesbachian and Dienerian Substages is relatively similar to other global sections, although, relative to the well-dated Arctic and Iranian sequences, the Griesbachian–Dienerian boundary appears to be lower, not unlike the situation in the Chinese Herchuan section.

However, the Tesero Horizon (basal Early Triassic Werfen Formation), which is the designated base of the Griesbachian in Italy, displays different polarities at the two sections sampled by Scholger *et al.* (2000). At Bulla, the Tesero Horizon is normal in polarity, whereas at Siusi, the Tesero Horizon displays reversed polarity (Scholger *et al.* 2000, figs 6 & 8). Sedimentation is argued to be continuous between the Permian Bellerophon and the Griesbachian Werfen Formations (see discussion by Scholger *et al.* 2000). However, the polarity difference of the Tesero Horizon between two sections only 8 km apart appears to suggest otherwise. Scholger *et al.* (2000) did not discuss this polarity difference in the Tesero Horizon results, but they claimed that their data supported the concept of continuous deposition between the Bellerophon and the Werfen formations. In fact, they refer to the Tesero Horizon as a synchronous 'boundary

event horizon'. But, the difference in polarities indicates that either the Tesero beds are not a synchronous horizon between these two neighbouring sections, or that the remanent magnetization of at least one of the sections does not represent the geomagnetic field at the time of Tesero deposition.

In an attempt to investigate this issue further, the magnetic study of the Gartnerkofel core (Zeissl & Mauritsch 1991) was re-examined. Examining the inclination data, the polarity was interpreted very stringently, that is, only the normal or reversed polarity results clearly fitting the palaeogeographic location of the locality at the time of deposition were considered. This stringent polarity interpretation suggests that the upper part of the Tesero Horizon above the black clay layer at the Gartnerkofel core site has reversed polarity, while the lower part has normal polarity, but a direction that resembles that of the recent geomagnetic field and thus may be a recent secondary magnetization. However, of far greater significance, the data from the entire core displayed far more reversed polarity than is known for the Early Triassic – Late Permian time interval, suggesting the possibility that a reversed-polarity secondary magnetization may have overprinted the strata cored. These complications prevented the issue of the polarity of the Tesero Horizon from being determined from the core data. Therefore, the problem remains that the differences between the Bulla and Siusi sections suggest that the Tesero between Bulla and Siusi is not a synchronous horizon or has been remagnetized in at least one section.

The uppermost Permian strata also are different between the two sections. At Bulla, only the uppermost beds of the Permian Bellerophon Formation beneath the Tesero Horizon, ~1.7 m thick, were sampled (probably because that was the extent of the available exposure in the roadcut); these beds display reversed polarity, consistent with most Late Permian sections globally. In the natural outcrop at Siusi, the Tesero Horizon and underlying uppermost 0.5 m of the Bellerophon Formation showed noisy, reversed polarity. Below, another ~15.5 m of Bellerophon strata were sampled and displayed only normal polarity; however, these normal polarity samples exhibit a slightly different palaeomagnetic direction than that of the normal polarity samples in the overlying Werfen Formation. If the magnetizations at both sections are original magnetizations dating from deposition of the strata, the normal polarity of the Bellerophon strata at Siusi (except for the uppermost 0.5 m) and reversed polarity of the uppermost 1.7 m at Bulla may indicate erosion of the uppermost Bellerophon strata beneath the Tesero Horizon. The issue of erosion has been much debated in the literature, with most authors presently considering that no depositional break exists. But, for these magnetic results to represent the original magnetization at the time of deposition, some strata must be missing at Siusi, or alternatively, the Tesero Horizon at Siusi has been remagnetized. Even so, the distinctive reversed polarity of the Late Changhsingian (discussed in the following Permian section) is missing at Siusi.

A section in Albania investigated the uppermost Early Triassic and the early Mid- Triassic (Muttoni *et al.* 1996). The Spathian–Anisian boundary was studied in a fossiliferous marine sequence at Kçira (Fig. 1, column 6). The Spathian of the Kçira section is similar to that of the Arctic stratotype sequence. Recent revision of the conodont biostratigraphy of the Kçira section (Bachman & Kozur 2004) suggests that the Spathian–Anisian boundary lies within a short reversed interval (Fig. 1, column 6). The Kçira section represents the only complete sequence across the Spathian–Anisian boundary; in both the Arctic and the Chinese Herchuan sections, sampling stopped short of the boundary. North American terrestrial sections in Arizona and New Mexico (Fig. 1, columns 11 & 12) both sampled Anisian strata above an erosional unconformity. Only vertebrate fossils provide any age control, and vertebrate faunal age resolution presently is inadequate to determine whether the strata of these sections straddle the Anisian–Spathian boundary, begin at the boundary, or begin within the Anisian. However, comparison of these two North American sections with the Kçira section indicates that North American deposition probably began a bit above the Spathian–Anisian boundary.

### *China*

Only marine strata have been studied in China thus far; five marine sections in the Sichuan Basin on the South China Block sampled some portion of the Early Triassic. Early Triassic deposition at the Herchuan section (Fig. 1, column 1; Steiner *et al.* 1989) was in a marginal marine setting, whereas Late Permian strata were deposited in a wholly marine environment. The lower portion of the Early Triassic, the Feixianguan Formation, consists of alternating red and grey shales and limestones. The Feixianguan strata gave unambiguous palaeomagnetic polarity results. At the time of the study, the age of only the lower 100 m of the 400 m of Feixianguan strata were known; these contained Griesbachian

conodonts. The upper 300 m contain no age-diagnostic fauna, but conformably overlie the lower Feixianguan beds and are conformably overlain by the Jialingjiang Formation. Conodonts found throughout the 600 m of the Jialingjiang Formation were identified as long-ranging species of the Smithian–Spathian Substages.

The Jialingjiang strata consist of grey, thin-bedded limestones and brown dolomite. The dolomite has experienced considerable dissolution of interbedded evaporites. Solution breccia and appreciable vuginess in the dolomites resulted in a poorly preserved record of the geomagnetic field polarity, particularly in the upper part of the formation; the many hachured intervals in column 1 of Figure 1 indicate the poor quality of the record. Although the biostratigraphical age information at the time of the study was limited, comparison of the magnetic polarity results with other global sections suggests that the Griesbachian may extend considerably higher than the highest Griesbachian conodonts, and that the lower part of the Jialingjiang strata may actually be Dienerian. In other words, the lower Jialingjiang strata up to the two larger normal polarity intervals in the middle of the formation, which were thought to be Smithian–Spathian, may be Dienerian. Those two thicker normal polarity intervals and the overlying vuggy interval with poor or no data may represent the complete Smithian Substage. Despite the problems of the upper part of the Herchuan sequence, the fit of the preserved magnetostratigraphy with the pattern from other global sections is reasonably good.

The Shangsi section (Fig. 1, column 2) of the northern Sichuan Basin has been sampled twice, first by Heller *et al.* (1988), who sampled the Upper Permian Dalong Formation and a portion of the overlying Lower Triassic Feixianguan Formation. Shortly thereafter, Steiner *et al.* (1989) also studied this sequence because Chinese colleagues considered this to be a very important section and insisted upon additional sampling. Steiner *et al.* (1989) sampled the entire Upper Permian section overlying the Middle Permian Maokou Formation at this site, that is, the Wuchiaping and Dalong formations, as well as the exposed portion of the overlying Feixianguan strata. Both sampling teams found that the original magnetization was preserved in only a portion of the samples in the Permian part of the section. When the portions of the stratigraphy that lacked stable magnetization (Fig. 1, column 2: diagonal lined areas in each of the sections) are taken into account, the resulting magnetostratigraphies are notably similar. Both indicate a basal normal polarity interval in the Feixianguan Formation overlain by reversed polarity, and the uppermost Changhsingian beds have reversed polarity in both studies.

Heller *et al.* (1995) sampled two sections in central Sichuan located near one another, Wulong and Shuijiang (Fig. 1, columns 4 & 5). The Upper Permian formations were sampled at Wulong, but because of better exposure and less weathering near the boundary, and the Lower Triassic Feixianguan Formation sampled at Shuijiang; the results were then combined into a single polarity sequence (Heller *et al.* 1995). However, Steiner *et al.*'s (1989) Liangfenya section is located very close to the Wulong section of Heller *et al.*; Steiner *et al.* noted that the Permian–Triassic boundary was a tectonic boundary in this area. Boudinage structures in the clay layer at the boundary indicate that slip has occurred along this horizon during a folding episode in that area. Two factors, the proximity of the Wulong section to that the Liangfenya section and reversed polarity characterizing the Lower Triassic lower Daye Formation at the Wulong section, suggest the tectonic disruption of the stratigraphic sequence was even greater at the Wulong outcrop, because the lowest Triassic strata are always normal in polarity elsewhere. For these reasons, a large hiatus is shown in the Wulong section in Figure 1 (column 4). Although the Shuijiang section also is near the Liangfenya and Wulong sections, the Shuijiang section shows the standard polarity pattern of the Early Triassic sequences elsewhere, suggesting a lack of disruption of the stratigraphic section there.

### *Africa*

The location of the Permian–Triassic boundary is not precisely known within the terrestrial Karoo Group strata, because there are two possible indicators of the extinction event. Vertebrate remains indicate a faunal change from the Permian *Dicynodon* to the dominantly Triassic *Lystrosaurus*, but their ranges overlap (Smith 1995). An abundance of fungal/algal remains is present in the Karoo Supergroup (Steiner *et al.* 2003), and this horizon presents another biostratigraphic indicator of the Permian–Triassic boundary. Furthermore, although the magnetostratigraphy of the Karoo Supergroup has been studied in several locations (Schwindt *et al.* 2003; de Kock & Kirschvink 2004; Ward *et al.* 2005), different conclusions have been reached. Schwindt *et al.* (2003) studied the magnetostratigraphy throughout the Upper Permian and lowest Triassic strata at the locality in which the fungal horizon was found; only magnetizations strongly overprinted by Early Jurassic Karoo

igneous activity were observed. Much of the magnetization was either normal Jurassic polarity or multicomponent, unstable magnetization (Schwindt *et al.* 2003). The unstable multicomponent magnetization was commonly observed in green mudstone strata, which constitute most of the section; isotopic data (Tabor & Schwindt pers. comm.) suggest that the area may have been a swamp environment during deposition. The reducing geochemical environment within a swamp would explain the paucity of stable remanent magnetization in much of the strata, because of the dissolution of magnetic carriers under these conditions. Carbonate nodules also were collected in an attempt to locate the Permian–Triassic boundary by its delta-$C^{13}$ anomaly, but the nodules gave only a recent climatic signature.

Subsequently, Ward *et al.* (2005) published a magnetostratigraphic interpretation for part of Schwindt *et al.*'s (2003) section, but without any supporting palaeomagnetic data. Column 9 of Figure 1 is their interpretation of the magnetostratigraphy; they indicated the relative positions of the change in vertebrate faunal change ('V' in column 9) and their interpretation of the location of Steiner *et al.*'s (2003) fungal horizon ('F' in column 9). These potential Permian–Triassic boundary markers do not coincide, therefore the Permian–Triassic boundary position in the Karoo strata still is not precisely known, although both potential Permian–Triassic boundary markers apparently lie within the lower portion of the Griesbachian normal polarity interval recognized globally. Based on the fact that the marine Permian–Triassic boundary indicator, the FAD of the conodont *Hindeodus parvus*, lies about one third of the distance above the base of the Griesbachian normal polarity interval, the fungal spike may most accurately represent the Permian–Triassic boundary in the Karoo Group.

### *Early Triassic polarity: summary*

Figure 1 suggests that Early Triassic geomagnetic polarity was slightly dominated by reversed polarity; normal polarity intervals occur within the more extensive reversed polarity and form a distinctive pattern, identifiable in most of the sections and providing good correlation among them. Four distinctive portions of the Early Triassic polarity pattern repeat in the global magnetostratigraphic sequences; these are highlighted by different colours in Figure 1 and labelled according to the characteristic polarity of the interval and the substage that each occupies: 'Gries N', 'Diener R-N', 'Smith N', and 'Spath N'. Very latest Late Spathian time probably began in the 'Anis N1' interval.

Originally, the base of the Triassic was considered to be the base of the Griesbachian Substage (Tozer 1967), but now, based on more refined conodont zonations, the lower portion (one third) of the Griesbachian Substage is thought to be Late Permian. The Griesbachian Substage of the Arctic stratotype contains normal polarity in its lower part (Ogg & Steiner 1991), corresponding to the Gries N interval of Figure 1. Following this normal polarity interval, the Upper Griesbachian and Dienerian display a distinctive interval of reversed polarity punctuated by a number of shorter normal polarity intervals; this is the interval Diener R-N. Many of the sections display three to four relatively short normal polarity intervals, although other sequences suggest the possibility of more. Overall, the Griesbachian and Dienerian Substages of Tozer (1967) are comprised of a normal interval overlain by a dominantly reversed interval in which three or more relatively short normal polarity periods are interspersed. In the stratotype sequence, the Smithian Substage is dominantly of normal polarity (Fig. 1: Smith N); Smith N begins near the base of the Smithian and persists for most of the duration of the Smithian. The Lower Smithian boundary of the stratotype section begins near the polarity boundary between Diener R-N and Smith N. A reversed polarity interval of relatively long duration existed during the Late Smithian through the early half of the Spathian. In the Mid-Spathian, the polarity changed to normal; the upper half of the Spathian is characterized by slightly shorter normal and reversed intervals. In the stratotype section, normal polarity resumes before the end of the Spathian.

## The Late and Middle Permian

An even larger number of magnetostratigraphic sequences have been studied in Upper and Middle Permian strata (Fig. 2) than in Early Triassic beds. Chinese strata contain the Late Permian (Lopingian) global stratotype, whereas the Middle Permian (Guadalupian) stratotype is in the United States. Figure 2 includes, in addition to the marine and terrestrial sedimentary sequences, the igneous sequences of the Siberian Traps and Emishan Basalt.

In general, Permian magnetostratigraphic sequences do not agree well. However, most of the sedimentary sections show that a relatively short duration of reversed polarity characterized the very latest Changhsingian Stage, preceded by a longer duration interval of normal polarity.

A hiatus near the Permian–Triassic boundary is described or discussed in the section descriptions from the western Tethyan magnetostratigraphic investigations in Pakistan and Italy, but no allowance for a hiatus was made in the published polarity interpretation columns. In Figure 2, inferences of missing time have been added from the lithological descriptions and inferences from the magnetostratigraphy.

### *China*

Five marine sections (Fig. 2, columns 3–6), one marginal marine (column 7), one terrestrial (column 2), and one basalt section (column 1) have been studied in China. One of the marine sections, the Liangfenya section, is not shown in Figure 2, because it is depicted in Figure 1 and has only minor data content and because of the space constraints of Figure 2. Most of the Chinese sections show that normal polarity prevailed in the lower Griesbachian Substage. Generally, Changhsingian-age beds indicate that a reversed polarity interval of relatively short duration preceded the Early Griesbachian normal polarity. Below this relatively short reversed interval, a considerably longer period of normal polarity commonly is observed. The oldest polarity signature in the marine Chinese sections is an even longer duration of reversed polarity, occupying the Wuchiapingian Stage (*not* formation). But, within this lengthy Wuchiapingian reversed interval, the Linshui (Heller *et al.* 1995) and the Shangsi (Steiner *et al.* 1989) sections indicate the presence of another (shorter) normal polarity interval. In the GSSP Meishan section, a very brief reversed-polarity interval was observed (Liu *et al.* 1999; Zhu & Liu 1999); this reversed polarity is not observed in any other Permian–Triassic sequence. Bachman & Kozur (2004) state that this interval of the Meishan section was restudied, and the reversed polarity was concluded to be an overprint (see Bachman & Kozur 2004, pers. comm. by Yin Hongfu to Kozur).

The non-marine Taiyuan sequence (Embleton *et al.* 1996) has no firm age control, but is reported to lie conformably between Upper Carboniferous to Lower Permian strata and Lower Triassic strata. Because the sequence is reported to contain no breaks in sedimentation, Embleton *et al.* (1996) approximated ages for it by assuming a uniform sedimentation rate. Their interpretation indicates that the earliest normal polarity stratigraphic horizons (U Shihezi Formation Member A) are in the earliest Middle Permian, essentially in the Roadian and approximately middle Wordian. However, the dominance of normal polarity in the lower and upper parts of this undated sequence most resembles the upper and lower normal polarity intervals observed globally in the Middle and Upper Permian. Therefore, in Figure 2, the Taiyuan section has been uniformly compressed in an attempt to make it fit the global pattern; the fit is not outstanding, suggesting that sedimentation rates were not constant. But, this representation of the approximate age of the Taiyuan section makes its polarity sequence agree moderately well with the global pattern.

The magnetostratigraphy of the Emishan basalts is shown in Figure 2, column 1; the basalts exhibited a lengthy normal polarity interval succeeded by reversed polarity (Huang & Opdyke 1998; Fig. 2, column 1). The basalts lie disconformably on Maokou limestones (Capitanian–Kazanian age: Huang & Opdyke 1998; Lo *et al.* 2002) and are overlain by the Changhsingian age Xuanwei Formation. Recent $Ar^{40}/Ar^{39}$ dating of the basalts indicated that they are 251–253 Ma (Lo *et al.* 2002). Lo *et al.* (2002) also argued that the proximity of the Emishan basalts to the Late Permian to Early Triassic marine strata of southern China was consistent with the Emishan extrusions being the source of the numerous tuffaceous beds in the southern China strata. However, U–Pb dating of a sill intruding the Emishan basalts gave a 259 Ma age for the intrusion, implying that the basalts are older than 259 Ma. The conflicting radiometric data make it difficult to correlate the Emishan basalt magnetostratigraphy with other Permian sequences. The basalts exhibit dominantly normal polarity, which could represent either the upper lengthy normal polarity interval of the Late Permian or the older normal polarity interval of the upper Middle Permian. The second correlation is shown in Figure 2 because of the possibly greater reliability of U–Pb radiochronometry.

### *Western Tethys*

Two sections were studied in the Late Permian of Iran (Fig. 2, column 10a & b; Besse *et al.* 1998; Gallet *et al.* 2000). A Middle and Upper Permian section was studied in Pakistan (Fig. 2, column 9; Haag & Heller 1991). The Pakistan section subsequently has been dated in detail with conodont biostratigraphy (Wardlaw & Pogue 1995). In Italy, three localities in Permian strata have been investigated (Zeissl & Mauritsch 1991; Scholger *et al.* 2000), but only the Dolomites sequences (Scholger *et al.* 2000) gave reliable data (Fig. 2, column 8).

Both the Iranian and Pakistani sequences display reversed polarity in the uppermost Changhsingian, interrupted by a very short normal event (Fig. 2, columns 9, 10a & b). Both show that this triplet of R-N-R succeeded a lengthier normal polarity interval. In China, this normal polarity interval is within the Changhsingian Stage, but in Iran Krystyn dated it with conodonts (Gallet *et al.* 2000) as Dorashamian. Wardlaw & Pogue (1995) also identified sequence stratigraphical horizons indicating transgressions and regressions in this section; these sequence boundaries are shown by green lines in Figure 2, column 9.

The two sections in the Italian Dolomites (Scholger *et al.* 2000) have already been discussed; the results were differing magnetic polarity for the Tesero Horizon and the upper Bellerophon Formation from these sections located 8 km apart. The minimal exposure of the Permian Bellerophon Formation at the possibly more reliable Bulla section yielded 1.7 m of reversed polarity below the normal polarity of the Tesero Horizon (Fig. 2, column 8: T in yellow) and Mazzin Member of the lower Werfen Formation. This magnetostratigraphy is consistent with sections globally. The *c.* 16 m of upper Bellerophon strata sampled at the Siusi outcrop exhibit normal polarity, but with a direction slightly different from the overlying Werfen Formation normal polarity at this section. Column 8 of Figure 2 displays the Siusi Bellerophon results below those of Bulla (after scaling for an apparent difference in sedimentary accumulation between the two sections). The amount of reversed section sampled at Bulla is too little to represent the whole short reversed interval of the Late Permian that is indicated by most global magnetostratigraphic results, therefore, a hiatus was placed between the Bulla and Siusi Bellerophon results in column 8 of Figure 2. Erosion of the uppermost Bellerophon Formation at Siusi by the 'current event' (Dolomites-wide erosion event) discussed by Scholger *et al.* (2000) would explain the differences in the Permian Bellerophon strata between the two localities and make the Dolomites results compatible with global Permian sections.

## *North America*

Two sequences of Late and Middle Permian strata in North America have been studied magnetostratigraphically, those in Texas–New Mexico (Fig. 2, column 13) and in Wyoming (Fig. 2, column 15). Both consist of terrestrial red beds interbedded with marine carbonates.

In Texas, the uppermost Permian formation, the Quartermaster Formation (also widely known as the Dewey Lake Formation, a name proposed somewhat later), has been investigated. The formation is truncated everywhere by the Late Triassic Santa Rosa Formation, hence Quartermaster sections vary appreciably in thickness from one location to another. The thickest outcrop section known is that in Caprock Canyon State Park, studied in its lower part by Molina-Garza *et al.* (1989) and in its entirety by Steiner & Renne (1996). Molina-Garza *et al.* (1989) observed four polarity intervals in the lower 32 m. Steiner & Renne (1996) sampled the same section more densely every 0.1 to 0.5 m throughout the entire 93 m; the results were largely normal polarity, but punctuated by three distinct, short reversed polarity intervals (Fig. 2, upper column 13). Two volcanic ash beds are present in the lower part of the Dewey Lake beds, separated by 20 m of fine-grained red sediment. Preliminary $^{40}Ar/^{39}Ar$ dating gave ages of ~250 Ma for each ash bed; however, the zircon populations show evidence of detrital contamination (Renne *et al.* 1996; Steiner & Renne 1996, 1998; Steiner 2000; Steiner 2001*a*, *b*). A short section (22 m) in the middle part of the same sequence, but with only one ash bed, was sampled 120 km to the south, and the same magnetostratigraphy was observed (Steiner 2001*a*, *b*). Beneath the Dewey Lake beds (4 m below the lower ash bed), lie frequently alternating beds of anhydrite and red siltstone, locally called the Alibates Beds, forming the lower part of the Quartermaster Formation. The Alibates Beds exhibited entirely reversed polarity with the exception of a short normal polarity interval within the lower part of the reversed polarity (Steiner 2001*a*, *b*).

In the subsurface of the sampling area, the Dewey Lake Formation overlies the Rustler Formation. Much farther south (southeastern New Mexico), the Dewey Lake Formation overlies the Rustler Formation in outcrop. Molina-Garza *et al.* (2000) sampled the Dewey Lake beds and observed dominantly normal polarity with one short reversed polarity interval in approximately the middle of the normal polarity. No ash beds were observed by Molina-Garza *et al.* (2000).

The underlying Rustler Formation consists of five members of alternating red beds and dolomite. The fourth member from the base, a 12 m thick dolomite, was studied in five sections (Steiner 2001*a*, *b*). The dolomite exhibited dominantly reversed polarity with a short normal interval in the upper part (Steiner 2001*a*, *b*). Palaeogeography of the Permian Basin during

the Late Permian consisted of the sea to the south and terrestrial environments to the north, west and east. Because both bedded anhydrite and dolomite require standing water from which to precipitate, it is probable that the interbedded anhydrite and red beds of the Alibates Beds below the Dewey Lake beds in northern Texas are the lateral equivalent of the interbedded dolomite and red beds of the Rustler Formation lying below the Dewey Lake in southwestern Texas–New Mexico. Both probably represent frequent marine incursions of the sea into the terrestrial depositional environment; that is, they probably represent deposition during approximately the same time period. Moreover, the same magnetostratigraphic signature is displayed by both sets of strata underlying the Dewey Lake Formation. The Alibates Beds and the upper Rustler Formation exhibit very similar magnetostratigraphies: dominantly reversed polarity encompassing a short normal polarity interval. On these bases, Steiner (2001*a*, *b*) concluded that the Alibates Beds and the Rustler Formation are likely to be lateral equivalents.

Below the Rustler Formation lies the thick, laminated (varved?) anhydrite sequence of the Castile Formation. Strata below the Castile Formation are the back-reef facies time equivalent of the reef and fore-reef facies that make up the global stratotype section for the Middle Permian. Reconnaissance sampling was conducted in the Castile evaporites and in the underlying back-reef facies formations: the Tansill, Yates, Seven Rivers, Queen and Grayburg formations, and the Cherry Canyon Member of the San Andres Formation. Short intervals in each of the formations were studied to assess suitability for palaeomagnetic investigation; much of the back-reef strata gave reliable palaeomagnetic results (Steiner, unpub. data).

Much earlier, Peterson & Nairn (1971) had studied sites in the Middle and Late Permian of Oklahoma and Texas–New Mexico; they investigated sites in stratigraphical equivalents of the Quartermaster Formation, the Elk City and Cloud Chief formations, a site in the New Mexico Yates Formation, three sites in the Seven Rivers Formation, and sites in the Oklahoma terrestrial equivalents of the San Andres Formation (Blaine, Flowerpot, Hennessey, and Wellington formations). Peterson & Nairn's (1971) study was only concerned with obtaining palaeopole positions; they did not sample for magnetostratigraphy. Thus, they sampled only short stratigraphical intervals of one to several metres per site, and did not specify the stratigraphical locations of their sampling sites within the formations, nor the stratal thickness sampled. Nevertheless, their polarity results have been widely quoted in the search for the beginning of geomagnetic field reversals after the lengthy duration constant polarity of the Carboniferous–Permian. Both their results and those of Steiner (unpub. data) are displayed in column 13 of Figure 2, although the stratigraphic positions of Peterson & Nairn's (1971) polarity results are relatively arbitrary; column 13 displays Texas–New Mexico formation names on the left and Oklahoma names in italics on the right.

Below the Rustler Formation, a single hand sample from the underlying Castile was investigated; surprisingly however, definite Permian reversed polarity was observed (Steiner, unpub. data). The Tansill Formation below was sampled almost in its entirety in a roadcut, but it was only weakly magnetized. Some suggestions of reversed polarity were observed, but at this locality, the formation appears to retain little of an original magnetic signature. The very top of the underlying Yates Formation, at the Yates/Tansill contact, exhibited definite normal polarity; a roadcut site in the middle of the formation was generally poorly magnetized, but a few samples displayed reversed polarity. Peterson & Nairn's (1971) single site in the Yates yielded normal polarity; the minimal outcrop description and the absence of coring holes at either of Steiner's sites suggests that Peterson and Nairn's locality was not the same location as the present author's Yates/Tansill contact site. Therefore, Peterson & Nairn's (1971) result is arbitrarily placed lower within the formation in Figure 2 (the lower normal polarity shown in the Yates Formation in column 13), although it could be almost anywhere in the formation.

Peterson & Nairn (1971) and Steiner (unpub. data) both sampled the Seven Rivers Formation. Steiner (unpub. data) sampled two duplicate short stratigraphical sections (4.5 m) about 6 m above the base of the formation in a roadcut; these exhibited a magnetostratigraphy of 1.6 m of normal polarity, overlain by 3 m of reversed polarity. Peterson & Nairn (1971) sampled three sites at one locality in the Seven Rivers Formation and obtained only reversed polarity; their result is represented by the lower Seven Rivers reversed polarity in Figure 2, which again, could be stratigraphically anywhere within the formation.

The uppermost Queen Formation, at its contact with the Seven Rivers Formation, displays reversed polarity magnetization over 3 m (Steiner, unpub. data). A continuous exposure, consisting in part of roadcuts, exposes the lowest Queen Formation through the upper half of the

Grayburg formations. The lowermost Queen Formation, at its contact with the underlying Grayburg Formation, contains a reversed to normal polarity sequence. The uppermost part of the Grayburg Formation is a light grey limestone/dolomite and is surprisingly well magnetized (Steiner, unpub. data); the upper 18 m display reversed polarity. The lower part of the Grayburg Formation, overlying the Cherry Canyon Sandstone Member of the San Andres Formation, is exposed on a hill slope. The Grayburg beds have a yellowish hue on the natural outcrop; the lowest 21 m generally exhibited relatively poor magnetization. However, a number of samples indicate the presence of a low-inclination normal polarity magnetization; because of the poorer quality of the magnetization, it cannot be certain whether this normal polarity dates from deposition without further investigation. Therefore, the normal polarity observation is shown as half bars of polarity among the diagonal-ruled pattern indicating poor data in column 13 (Fig. 2). The directly underlying Cherry Canyon Member of the San Andres Formation yielded indecipherable data throughout ~19 m (Steiner, unpub. data). However, Peterson & Nairn (1971) sampled San Andres-equivalent terrestrial strata in Oklahoma; their sites in the Blaine, Flowerpot, Hennessey, and Wellington formations yielded only reversed polarity (Fig. 2, column 13). Furthermore, magnetostratigraphic sequences of many tens of metres at both the top and bottom of the several hundred metres thick Blaine Formation of western Texas also recorded only reversed polarity (Steiner, unpub. data).

The Wyoming Permian–Triassic sequence has been studied in magnetostratigraphic reconnaissance from the lowermost Triassic down through 75 m of Permian strata; the investigation was conducted 48 km west of Laramie, Wyoming, as part of several palaeomagnetic class projects. In western Wyoming, the Permian section consists of limestones, shales, and cherts deposited in the Phosphoria seaway that covered western Wyoming, Idaho, Montana, and Utah in the Middle and Late Permian, the result of which was the deposition of the Phosphoria Group. Much of Wyoming east of the sea was a broad flat region on which red-bed deposition took place, but which was occasionally was invaded by marine waters, creating a stratal succession of intertonguing red beds and marine carbonates and gypsum: the Goose Egg Formation. Conodonts and gastropods in the marine Phosphoria Formation indicate an age of Middle Permian, Roadian through earliest Capitanian (Wardlaw & Collinson 1986). The highest Phosphoria beds are overlain by marine shale of the Griesbachian Dinwoody Formation. Hence, a gap must exist in western Wyoming between the lower Capitanian uppermost Phosphoria (Wardlaw & Collinson 1986) and the Griesbachian Dinwoody beds (Paull & Paull 1986).

Eastward in the dominantly terrestrial strata, no indication of a physical break can be found between the Goose Egg and overlying Triassic Red Peak formations, and the Permian–Triassic boundary cannot be identified in this area, in either surface exposures or subsurface data. In fact, a thesis was aimed specifically at locating the Permian–Triassic boundary in these strata, by measuring gamma ray stratigraphy on outcrop and correlating the results with the gamma ray logs of subsurface wells (Renner 1988; Renner & Boyd 1988). Renner was unable to find any evidence of a depositional break, and he concluded that no significant break in sedimentation existed, but that possibly extensive deposition of loess, perhaps containing a number of small breaks in sedimentation, might explain the apparent continuity.

The largely Permian Goose Egg Formation and lowermost part of the Triassic Red Peak Formation were sampled magnetostratigraphically at Renner's (1988) Red Mountain section in southeastern Wyoming. Approximately 80 m of stratigraphic section have been sampled in part, from the top of the locally named 'Blaine Gypsum' into the lower beds of the Red Peak Formation. Red-bed strata and three carbonate members were sampled, all of which gave clearly defined magnetic data and unambiguous polarity interpretations; the summary of these data is shown in column 15 of Figure 2. Although the magnetic stability was excellent, the ages of these strata are embarrassingly poorly known. The age of the Goose Egg Formation had been assigned by lateral tracing of the carbonate tongues into the main body of the Phosphoria Formation. (e.g. Thomas 1934). However, outcrop exposures between that wholly marine province and that of dominantly terrestrial deposition are not continuous; therefore, the exact connections are not well established and, in some cases, have been much debated (Boyd & Maughan 1973). It was hoped that the magnetostratigraphic results would help to remove some of the age uncertainties, by allowing magnetic correlation of the Goose Egg strata to better-dated Permian strata.

At the sampling locality, the *c.* 6 m of lowermost Red Peak Formation red beds displayed normal polarity, and they rest directly on gypsum at the top of the Little Medicine Member of

the Goose Egg Formation; *c.* 2 m of gypsum overlying *c.* 2 m of dolomite constitute the Little Medicine Member. The dolomites exhibit reversed polarity. The age of the Little Medicine Member has been argued to be Late Griesbachian from lateral tracing into the top of the Dinwoody Formation of western Wyoming (Thomas 1934). However, subsequently it has been argued (Paull & Paull 1990) that the Little Medicine Member is not physically continuous with the Dinwoody strata. The Little Medicine Member has no fauna, so its age really is not known, only hypothesized. Beneath its dolomite lie fine-grained red beds of the Freezeout Member.

The Freezeout red beds also have no age control. They exhibited well-defined normal polarity in the portion sampled. Interbedded dolomite, gypsum and red beds of the Ervay Member underlie the Freezeout Member; the Ervay dolomites can be traced laterally into the Ervay Member of the marine Park City Formation. The Ervay Member forms the top of the Park City Formation, and therefore the top of the Permian in western Wyoming. The Ervay Member is directly overlain by the Griesbachian Dinwoody Formation. Wardlaw & Collinson (1986) found that the highest Ervay beds of the Park City Formation contain conodonts of late Wordian to early Capitanian age; however, Henderson & Mei (2000) reviewed provinciality in conodont identifications and questioned the identification of certain conodonts in the upper Ervay strata, suggesting that these beds may be as young as Lopingian. In a later publication, Wardlaw (2003) stated that those conodonts are late Wordian.

The Ervay Member exhibits largely reversed-polarity magnetization, but changes to normal polarity in its lowest portion. The normal polarity continues in the underlying fine-grained Difficulty Member red beds. Below the Difficulty red beds, another marine tongue, the Forelle Member, gave reversed polarity for the portion sampled; the Forelle Member is traced into Wordian strata of the Park City Formation. The underlying Glendo Member red beds were sampled in their middle portion, and these displayed normal polarity overlain by reversed polarity. The base of the Glendo Member was also sampled, down to the top of a 20-m-thick gypsum deposit, the local 'Blaine Gypsum'. Whether this gypsum correlates to the type Blaine gypsum of Oklahoma and Texas has not been established, but it does occur at approximately the same stratigraphical position in the Wyoming sequence as the Blaine Formation in the Texas and Oklahoma sequences. Moreover, comparison of the magnetostratigraphic results from the entire Wyoming section between the Blaine gypsum and the Red Peak red beds with the global results appears to suggest that the Wyoming Blaine gypsum is correlative with the Texas–Oklahoma Blaine Formation.

The magnetostratigraphy of the succession exposed in southeastern Wyoming is combined with the composite of entire Early Triassic Red Peak Formation from its contact with the Dinwoody Formation of western Wyoming to the Alcova Limestone in column 15 of Figure 2; the juncture between the western and southeastern Wyoming sections is marked with an unsampled interval by a '?', because the exact correlation has not been studied. The incomplete magnetostratigraphic results from the southeastern Wyoming Permian section display three prominent normal polarity intervals between the base of the Red Peak Formation there and the top of the gypsum. Despite the poor age control, these normal polarity intervals are located in positions similar to, and with similar thicknesses (possibly indicating comparable durations), to the normal polarity intervals observed in the global collection of Middle and Late Permian sequences of Figure 2.

The positions of these normal polarity intervals below the Red Peak Formation suggest that the Little Medicine and Freezeout members of the Goose Egg Formation of southeastern Wyoming are Late Permian in age, and not Early Triassic as has been supposed. The correlation suggests that the Little Medicine Member represents the uppermost Changhsingian in Wyoming, and the Freezeout Member represents the lower Changhsingian. Other correlations between the Wyoming Permian and Triassic composite and the global results, based on the locations of these normal polarity intervals, have been tested, but that shown in Figure 2 provides the best fit of the magnetostratigraphy and the limited biostratigraphy. However, the biostratigraphy of the upper portion is significantly at odds with the global data, and may suggest that Henderson & Mei's (2000) conodont identifications are correct. The field of conodont identification has undergone much revision since 1986. If the magnetostratigraphic correlation is correct, the polarity sequence certainly permits the possibility of relative continuity of deposition across the Permian–Triassic boundary in southeastern Wyoming that Renner (1988) concluded.

### *Russia and Transcaucasia*

An extremely large number of Upper Permian magnetostratigraphic sections have been studied

in Russia, largely in terrestrial red-bed sequences; five representative magnetostratigraphies columns are shown in Figure 2 (columns 16–20). Khramov has studied the Permian and Triassic magnetostratigraphy of Russia since 1960; his most recent summary (Khramov 1987) is shown in column 18 of Figure 2. Molostovsky (1983) has studied the eastern Russian Platform magnetostratigraphy extensively; his figure 20 is reproduced in column 16 of Figure 2 (beneath the summary of the Early Triassic by Lozovsky & Molostovsky 1993). Molostovsky's (1983) figure 20 is illustrated instead of his summary figure representing all of his studies of the Upper Permian, in order to show the fine-scale polarity details he observed in that sequence. These details are eliminated from his summary, but display the same fine-scale polarity details observed globally.

On Novaya Zemlya, Gurevich & Slautsitays (1985) investigated a sequence of strata that consists of grey marine clastics grading upward into variegated clastic rocks and into terrestrial red beds, without an observable break in deposition. Tuffs occur in the base of the variegated deposits and comparison of the magnetostratigraphy (Fig. 2, column 17) to global sequences suggests that the Permian–Triassic boundary lies at the base of the variegated deposits with their tuffaceous content.

The type Tatarian is a terrestrial section originally investigated by Khramov (1963). Recently, a portion of this sequence was restudied by Gialanella *et al.* (1997). The result of all investigations is displayed in column 20 of Figure 2. The lithologic subdivisions of the Tatarian are indicated by Roman numerals on the right side of the age column.

Kotylar *et al.* (1984) studied a marine sequence in Transcaucasia, the stratotype region for the Dorashamian and Dzhulfian, and at the location of the type Midian; the results are shown in column 19 of Figure 2. An identical magnetostratigraphy was published by Zakharov & Sokarev (1991), with the exception that the normal interval designated as basal Triassic in Kotylar *et al.*'s (1984) magnetostratigraphy is shown as uppermost Dorashamian. The Transcaucasian sequence displays normal polarity low in the Middle Permian, like the North American sequences.

### *Central European Basin*

The Rotliegend and Zechstein formations have been studied in Germany (Menning 1986, 1988) and in Poland (Nawrocki 1997). Fairly similar results were obtained by both studies (Fig. 2, columns 26 & 27). The frequent reversals observed by Menning (1980, 1988) in the uppermost Rotliegend, although incomplete, are similar to the short reversed intervals observed in Iran and western. Texas within the lengthy Changhsingian normal polarity interval (Fig. 2, columns 10 & 13). This correlation is suggested in Figure 2, but the uncertainty of its validity is indicated by numerous question marks. The limited magnetostratigraphic data do not allow a definite correlation of the Zechstein strata to the rest of the world. However, in the underlying upper Rotliegend beds, the Capitanian normal polarity interval appears to be well represented in both sequences. Neither sequence displayed any normal polarity below the Capitanian normal interval, normal polarity that would be correlative with that observed in a few Wordian-equivalent strata of other sequences. However, its absence might be due to a hiatus between the upper and lower Rotliegend strata, as hypothesized by Nawrocki (1997).

### *Permian polarity: summary*

Just prior to the Permian–Triassic massive extinctions, the latest Permian exhibits a distinctive polarity pattern: a short duration R-N-R. The uppermost Changhsingian strata of a number of magnetostratigraphic sequences exhibit this observed pattern, including the reliable and biostratigraphically well-dated Iran and Pakistan sections, as well as the Russian Platform sequences, including the type Tatarian section, and the German sequence (Fig. 2, columns 9, 10a & b, 16, 20 & 25). Other sections (Shangsi, Wulong, Meishan and Poland) also appear to display this polarity structure, although possibly compromised by either poor magnetic recording or inadequately-detailed sampling.

Most of the Middle and Upper Permian sequences exhibit three prominent normal polarity intervals: the Permo-Triassic 'Gries N', the Late Permian 'Chang N' and the Middle Permian 'Capitan N' (Fig. 2). The recognition of this common polarity sequence provides important correlation markers for the Middle and Late Permian. In addition, five shorter duration polarity intervals appear recurrently among the various sequences and, when recognized, provide potential for fine-scale correlations. These are highlighted by coloured lines in Figure 2 and labelled in decreasing age as 'P1' – 'P5'. P5 is the short normal interval already discussed in the latest Changhsingian R-N-R sequence. The relatively long duration normal polarity interval, Chang N,

immediately precedes the distinctive Changhsingian R-N-R interval; Chang N is observed in every Late Permian sequence. Within Chang N, the triplet of brief reversed-polarity intervals recorded in the Iranian and Texas sequences constitutes P4. Linshui may also preserve this triplet (Fig. 2, column 3), but many sequences display only one of two of these short reversed-polarity intervals. P3, a short normal interval in the Lopingian reversed polarity preceding Chang N, is observed in only a few sequences: Pakistan, Texas, Wyoming, and Germany. P2 is a brief reversed-polarity interval within Capitan N. P1 is a short normal polarity interval documented in 4–6 sections (Fig. 2).

The oldest normal polarity observed is in the Wordian. 'Word N' occurs in the Queen Formation (possibly also in the Grayburg Formation) of the Texas–New Mexico section, in the Russian Transcausian section, and in the North American Wyoming Goose Egg Formation; all three sections clearly exhibit a relatively short duration interval of normal polarity. Therefore, the oldest normal polarity lies very low in the Middle Permian, approximately in the middle to upper part of the Wordian Stage. This interval constitutes the earliest normal polarity of the geomagnetic field and terminates the ~ 50 million years of constant polarity of the Carboniferous and Early Permian Kiaman Reversed Polarity Superchron. Therefore, it presently appears that the 'Illawarra reversals' began in the middle–upper Wordian Stage.

The oldest normal polarity, the initiation of the Illawarra reversals, previously had been argued to occur in the early Capitanian (Menning & Jin 1998). However, no magnetostratigraphic data have ever been published from the Guadalupian global stratotype. The stratotype beds (the United States Permian Basin strata) have been heavily oil saturated, which consequently dissolved the magnetic carriers (Steiner, unpub. data); therefore, the Guadalupian stratotype is unlikely to ever yield a detailed magnetostratigraphic sequence. However, the strata deposited behind the reef, the backreef facies, have yielded good palaeomagnetic data (Peterson & Nairn 1971).

Menning & Jin (1998) based their conclusion that the Illawarra reversals began in the Capitanian on Peterson & Nairn's (1971) observation of normal polarity in the backreef Yates Formation and no normal polarity in any older strata. Correlation of the backreef strata with the biostratigraphically dated reef and forereef strata (Glenister *et al.* 1992) suggests that the age of the Yates Formation is probably Middle Capitanian. As discussed earlier, Peterson & Nairn (1971) did no magnetostratigraphy, only limited site sampling (commonly one site per formation) and their sites spanned a limited stratigraphic thicknesses ($\leq 1$ to 4 m). Peterson & Nairn (1971) sampled the Yates Formation at only one site. Consequently, the normal polarity they observed probably represents several metres or less from an unspecified stratigraphical location within a 130-m-thick formation. Therefore, the age of Peterson & Nairn's (1971) Yates normal polarity is constrained only as some level within the middle Capitanian Stage. Moreover, despite the fact that Peterson & Nairn's (1971) three sites in the underlying Seven Rivers Formation yielded only reversed polarity, a single site from very low in the formation yielded 1.6 m of normal polarity succeeded by 3 m of reversed polarity (Steiner, unpub. data).

## Age of the Siberian flood basalts

Many investigators have concluded or speculated that the Siberian igneous activity caused the end-Permian mass extinction (recently summarized by Kamo *et al.* 2003). Magnetostratigraphy of the Siberian basalts has been published from four widely spaced areas (Lind *et al.* 1994; Gurevich *et al.* 1995; Fedorenko & Czamanske 1997; Westphal *et al.* 1998), but the results do not agree well at all (see Westphal *et al.* 1998). The polarity data were correlated with the uppermost Permian and early Early Triassic (Westphal *et al.* 1998). However, the present compilation and summary of global Late Permian and Early Triassic magnetostratigraphic data (Figs 1 & 2) suggests a better correlation of Siberian flood basalt magnetostratigraphic results, and consequently significantly different ages for the igneous activity.

Early $^{40}Ar/^{39}Ar$ results suggested an earliest Triassic age for the Siberian basalts (see Kamo *et al.* 1996 for tabulation of all Siberian radiometric data). In an early magnetostratigraphic assessment, Lind *et al.* (1994) correlated the basal reversed interval in their study of the Siberian igneous rocks with the youngest reversed interval in the Permian (Fig. 2, column 3). The most recent magnetostratigraphic study (Westphal *et al.* 1998) followed this scheme in correlating the results of all four studies among themselves and to the Early Triassic polarity sequence (Fig. 3, lower right). Westphal *et al.*'s (1998) correlation also preserved relative section thicknesses, whereas this constraint was relaxed somewhat in creating the new magnetostratigraphic correlation, because it is not reasonable to expect that the same rates of extrusion will occur in all parts of a volcanic field, and especially in one this large.

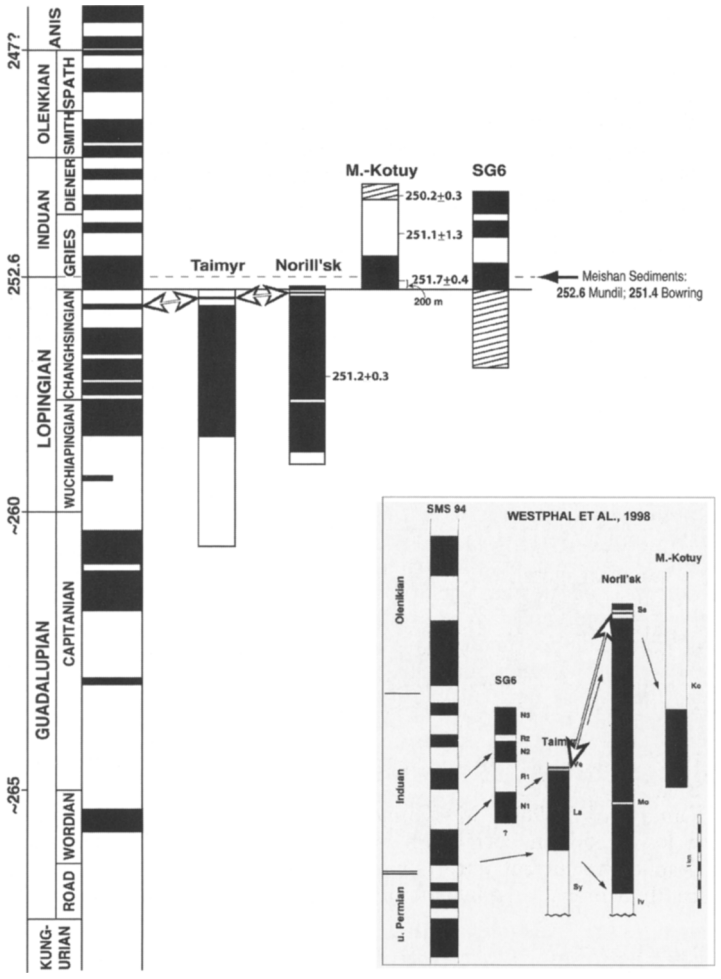


**Fig. 3.** The revised correlation of the magnetostratigraphy of the Siberian igneous episode and the Late and Middle Permian and Early Triassic magnetic polarity time scale derived by this study. The earlier magnetostratigraphic correlation of Westphal *et al.* (1998) is shown in the lower right. U–Pb radiometric ages (Kamo *et al.* 2003) for the igneous rocks are approximately in the stratigraphic positions indicated by Kamo *et al.* U–Pb dates determined for the Permian–Triassic boundary are on the right (Bowring *et al.* 1998; Mundil *et al.* 2004). Siberian magnetostratigraphy credits are listed in Figure 2. Normal (reversed) polarity is black (white); unsampled section indicated by diagonal lines.

The new magnetostratigraphic correlation is based on several characteristics of the Siberian igneous rocks that can be recognized as similar to features in the global Permian–Triassic magnetostratigraphic summary (Fig. 3, left side). Although the four studies were displayed in Figure 2 (columns 21–24), their characteristics are more clearly visible at the larger scale of Figure 3. In Westphal *et al.*'s (1998) correlation, the relationship of the SG6 sequence to the other sequences was considered problematic. As observed by Westphal *et al.* (1998), the SG6 sequence strongly resembles the Induan polarity sequence; however, the Taimyr and Noril'sk sections certainly do not.

One significant characteristic of the Siberian magnetostratigraphy is the record, in both the Taimyr and Noril'sk sections, of a very short normal polarity interval embedded within slightly longer duration, but also short, reversed polarity (Fig. 3, bold arrows). This signature is strikingly similar to that preserved in uppermost Changhsingian magnetostratigraphic sections, the interval 'P5' (Fig. 2). A second Siberian basalt

characteristic is the lengthy normal polarity interval below this short R-N-R sequence in the Taimyr and Noril'sk sections. No lengthy normal polarity periods like that occur in the Induan (Fig. 1), but a relatively long duration normal polarity interval is widely observed in the Late Permian (Chang N, Fig. 2).

Once the concept is considered that the four Siberian Trap magnetostratigraphic sections may not represent the exact same time interval (and indeed, their magnetostratigraphy suggests that they do not), the correlation shown in Figure 3 becomes the more probable. The two characteristics in the Taimyr and Noril'sk sections, of a short R-N-R succeeding a lengthy normal polarity interval, suggest that these sections are Late Changhsingian in age. The SG6 sequence is probably Induan, but could also represent extrusion spanning the Induan–Olenkian boundary. The Maimecha–Kotuy (M.-Kotuy) polarity sequence resembles the lower Induan (Griesbachian), particularly if either a hiatus or increased extrusion volume is responsible for the absence of the short normal polarity interval of the upper Griesbachian. However, the non-distinctive M.-Kotuy polarity sequence also resembles other parts of the time scale; the enormous thickness of reversed polarity displayed at M.-Kotuy (Gurevich *et al.* 1995) could suggest that the age of this sequence is early Lopingian. The detailed U–Pb dating of Kamo *et al.* (1996) at M.-Kotuy suggests that the lower Induan correlation is most probable, despite the current uncertainty in U–Pb dates recently demonstrated by Mundil *et al.* (2004).

This revised magnetostratigraphic correlation of the Siberian igneous rocks has enormous significance, in that it indicates that the Siberian flood basalt volcanism did not occur simply at the time of the mass extinction, but was ongoing in the Late Permian, that it spanned the Permian–Triassic boundary, and that it continued into the Early Triassic. The magnetostratigraphy of the Siberian flood basalts in Figure 3 suggests that the Siberian volcanism began in the late Guadalupian. Palaeontologists have long emphasized dual late Permian extinctions, one at the end of the Guadalupian and a second at the end of the Permian (see review by Erwin *et al.* 2002); it is possible that the Siberian volcanism also caused the end-Guadalupian extinctions, although the Emishan flood basalt volcanism may also have been active at similar times. Perhaps two separate pulses of Siberian volcanism caused the two separate mass extinctions, but with an appreciably larger eruption at the end of the Permian. The complication of Emishan volcanism erupting at similar times, and the presently sparse radiometric data, make it difficult to determine which was responsible or more responsible for the extinction events. The fact that both erupted in a similar time frame certainly affected the biosphere more than the Siberian activity alone; if the Emishan eruptions preceded those of Siberia, the Siberian flood basalt activity added environmental stress to an already stressed biosphere. Moreover, because the SG6 magnetostratigraphy indicates that volcanic extrusion continued through the early Early Triassic, the Siberian volcanism may also have been responsible for the slow Early Triassic faunal and floral recovery.

The magnetostratigraphy of the Siberian flood basalts indicates that the volcanism was not short-lived. Approximately eight geomagnetic field polarity intervals (ignoring the two short events) are observed. By the fast reversal rates of the late Tertiary, the magnetostratigraphically sampled part of the Siberian igneous rocks might represent ~1 Ma, but early Tertiary rates would imply 8 Ma. Comparison with the sparsely dated Permian–Triassic time scale indicates that the Siberian magnetostratigraphy represents ~9 Ma. Furthermore, geomagnetic field behaviour after constant polarity periods displays lengthy polarity intervals initially: the Late Cretaceous was characterized by polarity intervals of 4–6 Ma for the first *c.* 11 Ma after reversals resumed, succeeded by shorter polarity intervals of 1–2 Ma during the latest Cretaceous and early Tertiary and shorter still in the late Tertiary (*c.* 250 000 years). The Middle and Late Permian polarity intervals are 4 to 2 Ma, white the Early Triassic intervals are appreciably shorter.

The entire time spanned by the Siberian flood basalts may not yet have been sampled magnetostratigraphically; thus the estimated 8–9 Ma duration may be a minimum. Nevertheless, this magnetostratigraphic correlation of the Siberian rocks demonstrates that the eruptions of this greatest of flood basalt volcanism on Earth entirely overlaps in time with the greatest of mass extinctions. Therefore, Siberian basalt magnetostratigraphy strongly indicates that this massive flood basalt volcanism was causally related to the Permian–Triassic boundary mass extinctions. The prolonged volcanism probably was responsible for the biotic decline in the late Middle and Late Permian, probably by continual injection of excessive fluxes of carbon dioxide and hydrogen sulphide into the atmosphere.

The exact mechanism(s) by which the immense flood basalt volcanism affected the biosphere and produced mass death is beyond the scope of this investigation, but has recently been considered by others (e.g. Knoll *et al.* 1996;

Kump *et al.* 2005). In addition to periods of blocked sunlight due to dust and aerosols injected into the atmosphere and resulting temperature declines (volcanic winters), the excessive carbon dioxide delivered into the atmosphere could subsequently cause greenhouse conditions and overheating. Heating may have reached the point of warming the ocean waters to the extent that clathrates melted and released additional large quantities of carbon dioxide into the atmosphere. Finally, massive volcanic eruptions would inject lethal fluxes of hydrogen sulphide into the atmosphere, destined to return to the Earth's surface as acid rain. The fact that two large igneous provinces (Siberian and Emishan) operated partially at the same time and partially sequentially doubles the volcanic environmental devastation surrounding the time of the greatest of mass extinctions.

## Conclusions

The Early Triassic is characterized by four distinctive polarity intervals: Gries N, Diener R-N, Smith N and Spath N. The Upper and Middle Permian are characterized by two relatively longer duration normal intervals, Chang N and Capitan N, which are separated by two lengthy reversed-polarity intervals. Distinctive features of the Permian geomagnetic polarity time scale include a distinctive series of short reversed-normal-reversed polarity intervals in the uppermost Changhsingian and the earliest normal polarity in the Permian occurring in the Wordian Stage. The end of the 50 Ma of constant polarity in the Carboniferous–Permian is documented by three sequences as ending in the middle to late Wordian.

Correlations among the magnetostratigraphy of the large Siberian igneous province and with the composite Permian–Triassic magnetic polarity time scale developed in this study indicate that the Siberian volcanic activity not only spanned the Permian–Triassic boundary, but also began long before the end-Permian mass extinction and continued well into the Early Triassic. A total of at least eight polarity intervals are observed, suggesting that the duration of the volcanic activity may have been $\pm 9$ Ma. The Siberian magnetostratigraphic record suggests that volcanism began in the late Guadalupian and continued through the early half of the Induan. The age of the volcanism inferred from the magnetic polarity strongly suggests that the effects of the voluminous volcanic activity (carbon dioxide, hydrogen sulphide, etc.) disturbed the biosphere sufficiently to degrade the environment and to cause the mass extinctions. Magnetostratigraphy indicates that Siberian volcanism may have overlapped the latter stages of Emishan flood volcanism. Their essentially sequential activity must have delivered a one-two (or double) punch to the environment, and hence to the biosphere. Their close relationship in time leaves no doubt that the greatest extinction of advanced life on Earth was caused by abnormal volcanic activity.

This study also demonstrates that a magnetostratigraphy can be developed for the Guadalupian global stratotype sequence, despite the oil-saturated nature of the stratotype rocks. The extensive passage of oil through the reef and forereef facies, and the consequent dissolution of magnetic carriers, prohibits development of a magnetostratigraphy directly from the Guadalupian stratotype strata, thus excluding the stratotype beds from ever yielding a magnetostratigraphy to complement its excellent biostratigraphy. However, reconnaissance magnetostratigraphy of the backreef strata marginal to the reef–forereef stratotype rocks indicates good preservation of magnetization in many formations. Through correlations established between the backreef and reef–forereef strata, a magnetostratigraphic sequence could be determined for the Guadalupian stratotype, thus facilitating a more precise correlation of its fauna to other faunas globally. Therefore, the backreef strata should be investigated with detailed magnetostratigraphy.

The magnetostratigraphic summaries of this study also indicate that the southwestern North American Ochoan time period is not as short a time as has been hypothesized. Ochoan magnetostratigraphy duplicates much of the global Lopingian polarity sequence, therefore its duration is equivalent to nearly all of the Lopingian.

The intertonguing terrestrial–marine Permo–Triassic sequence in southeastern Wyoming may represent largely continuous sedimentation across the Permian–Triassic boundary. The uppermost Permian of this area probably is represented by the upper two members of the Goose Egg Formation (Little Medicine and the Freezeout Shale members). The magnetostratigraphic record obtained from the entire, poorly dated Wyoming Middle and Late Permian to Early Triassic strata (Goose Egg and Red Peak formations) matches the global time scale if the upper two members of the Goose Egg Formation are Upper Permian (Changhsingian), not earliest Triassic, as has been speculated for almost a century. Also, the 'Blaine Gypsum' of southeastern Wyoming occurs at the same magnetostratigraphic and stratigraphical position as the Blaine Formation of Texas–Oklahoma,

supporting long-time local speculation that this relatively thick gypsum deposit is approximately age equivalent to the Blaine Formation.

This work owes its existence to S. Lucas, who requested it and continually encouraged me when the task became overwhelming, as it frequently did. The very conscientious, constructive and detailed reviews by K. Ziegler and H. Közur greatly improved the quality of the manuscript and I sincerely and earnestly thank them. The study was supported by the Geology and Geophysics Department of the University of Wyoming.

## References

BACHMAN, G. H. & KOZUR, H. W. 2004. The Germanic Triassic: correlations with the international chronostratigraphic scale, numerical ages and Milankovitch cyclicity. *Hallesches Jahrbuch für Geowissenschaften, Reihe B*, **26**, 17–62.

BESSE, J., TORCQ, F., GALLET, Y., RICOU, L. E., KRYSTYN, L. & SAIDI, A. 1998, Late Permian to Late Triassic palaeomagnetic data from Iran: constraints on the migration of the Iranian Block through the Tethyan Ocean and initial destruction of Pangaea A. *Geophysical Journal International*, **135**, 77–92.

BOWRING, S. A., ERWIN, D. H., JIN, Y. G., MARTIN, M. W., DAVIDEK, K. & WANG, W. 1998. U/Pb zircon geochronology and tempo of the end-Permian mass extinction. *Science*, **280**(5366), 1039–1045.

BOYD, D. W. & MAUGHAN, E. K. 1973. Permian–Triassic boundary in the Middle Rocky Mountains. *In*: LOGAN, A. & HILLS, L. V. (eds) *The Permian and Triassic Systems and their Mutual Boundary*. Canadian Society of Petroleum Geologists; Memoir, **2**, 294–317.

CARR, T. R. & PAULL, R. K. 1983, Early Triassic stratigraphy and paleogeography of the Cordilleran Miogeocline. *In*: REYNOLDS, M. W. & DOLLY, E. D. (eds) *Rocky Mountain Paleogeography Symposium.* Society of Economic Paleontologists and Mineralogists Denver, **2**, 39–55.

DE KOCK, M. O. & KIRSCHVINK, J. L. 2004, Paleomagnetic constraints on the Permian–Triassic boundary in the terrestrial strata of the Karoo Supergroup, South Africa: implications for causes of the end-Permian extinction event. *Gondwana Research*, **7**, 175–183.

EMBLETON, B. J. J., MCELHINNY, M. W., MA, X., ZHANG, Z. & LI, Z. X. 1996. Permo-Triassic magnetostratigraphy in China: the type section near Taiyuan, Shanxi Province, North China. *Geophysical Journal*, **126**, 382–388.

ERWIN, D. H., BOWRING, S. A. & YUGAN, J. 2002. End-Permian mass extinctions: a review. *In*: KOEBERL, C. & MACLEOD, K. G. (eds) *Catastrophic Events and Mass Extinctions*: Impacts and Beyond. *Geological Society of America Special Paper*, **356**, 363–383.

FEDORENKO, V. & CZAMANSKE, G. K. 1997. Results of new field and geochemical studies of the volcanic and intrusive rocks of the Maymecha-Kotuy area, Siberian flood-basalt province, Russia. *International Geology Review*, **39**, 479–531.

GALLET, Y., KRYSTYN, L., BESSE, J., SAIDI, A. & RICOU, L.-E. 2000. New constraints on the Upper Permian Lower Triassic geomagnetic polarity time scale from the Abadeh section (central Iran). *Journal of Geophysical Research*, **105**, 2805–2815.

GIALANELLA, P. R., HELLER, F. *et al.* 1997. Late Permian magnetostratigraphy on the eastern Russian platform. *Geologie en Mijnbouw*, **76**, 145–154.

GLENISTER, B. F., BOYD, D. W. *et al.* 1992. The Guadalupian, proposed international standard for a Middle Permian series. *International Geology Review*, **34**, 857–888.

GRADSTEIN, F. M., OGG, J. G. & SMITH, A. G. 2004. *A Geological Time Scale 2004*. Cambridge University Press, Cambridge.

GUREVICH, YeL & SLAUTSITAYS, I. P. 1985, A paleomagnetic section in the Upper Permian and Triassic deposits of Novaya Zemlya. *International Geology Review*, **27**, 168–177.

GUREVICH, YeL, WESTPHAL, M., DARAGAN-SUCHOV, J., FEINBERG, H., POZZI, J. P. & KHRAMOV, A. N. 1995. Paleomagnetism and magnetostratigraphy of the traps from western Taimyr (northern Siberia) and the Permo-Triassic crisis. *Earth and Planetary Science Letters*, **136**, 461–473.

HAAG, M. & HELLER, F. 1991. Late Permian to Early Triassic magnetostratigraphy. *Earth and Planetary Science Letters*, **107**, 42–54.

HELLER, F., LOWRIE, W., LI, H. & WANG, J. 1988. Magnetostratigraphy of the Permo-Triassic boundary section at Shangsi (Guangyuan, Sichuan Province, China). *Earth and Planetary Science Letters*, **88**, 348–356.

HELLER, F., CHEN, H., DOBSON, J. & HAAG, M. 1995. Permian–Triassic magnetostratigraphy – new results from South China. *Earth and Planetary Science Letters*, **89**, 281–295.

HELSLEY, C. E. & STEINER, M. B. 1974, Paleomagnetism of the Lower Triassic Moenkopi Formation. *Geological Society of America, Bulletin*, **85**, 457–464.

HENDERSON, C. M. & MEI, S. 2000. Preliminary cool water Permian conodont zonation in north Pangaea: A review. *Permophiles*, **36**, 16–23.

HIGH, L. R. JR. & PICARD, M. D. 1967, Rock units and revised nomenclature, Chugwater Group (Triassic), western Wyoming. *Mountain Geologist*, **4**, 73–81.

HOUNSLOW, M. W., MORK, A., PETERS, C. & WEITSCHAT, W. 1996. Boreal Lower Triassic magnetostratigraphy from Deltadalen, central Svalbard. *Albertiana*, **17**, 3–10.

HUANG, K. & OPDYKE, N. D. 1998. Magnetostratigraphic investigations on an Emeishan Basalt section in western Guizhou Province, China. *Earth and Planetary Science Letters*, **163**, 1–14.

KAMO, S. L., CZAMANSKE, G. K. & KROGH, T. E. 1996 A minimum U-Pb age for Siberian flood-basalt volcanism. *Geochimica et Cosmochimica Acta*, **60**, 3505–3511.

KAMO, S. L., CZAMANSKE, G. K., AMELIN, Y., FEDORENKO, V. A., DAVIS, D. W. & TROFIMOV,

V. R. 2003. Rapid eruption of Siberian flood-volcanic rocks and evidence for coincidence with the Permian-Triassic boundary and mass extinction at 251 Ma. *Earth and Planetary Science Letters*, **214**, 75–91.

KHRAMOV, A. N. 1963. Paleomagnetic investigations of Upper Permian and lower Triassic sections on the northern and eastern Russian platform. *Trudy VNIGRI, Nedra, Leningrad*, **204**, 145–174. [In Russian]

KHRAMOV, A. N. 1987. *Paleomagnetology*. Springer-Verlag, Berlin.

KNOLL, A. H., BAMBACH, D. E., CANFIELD, D. E. & GROTZINGER, J. P. 1996. Comparative Earth history and the Late Permian mass extinction. *Science*, **273**, 452–457.

KUMP, L. R, PAVLOV, A. & ARTHUR, M. A. 2005. Massive release of hydrogen sulfide to the surface ocean and atmosphere during intervals of ocean anoxia. *Geology*, **33**, 397–400.

KOTYLAR, G. V., KOMISSAROVA, R. A., KHRAMOV, A. N. & CHEDIYA, I. O. 1984. Paleomagneitaya kharakteristika verkhnepermakikh otlozheniy Zakavkaz'ya. [Paleomagnetism of the Upper Permian Rocks of Transcaucasia.] *Doklady Akademii Nauk SSSR*, **276**(3), 669–674. [Translated by Scripta Technica.]

LIND, E. N., KROPOTOV, S. V., CZAMANSKE, G. K., GROMME, C. S. & FEDORENKO, V. A. 1994. Paleomagnetism of the Siberian flood basalts of the Noril'sk area: a constraint on eruption duration. *International Geology Review*, **36**, 1139–1150.

LIU, Y-Y., ZHU, Y-M. & TIAN, W-H. 1999. New magnetic results from Meishan section, Changxing County, Zhejiang Province. *Earth Science, Journal of China University of Geoscience*, **24**(2), 151–154.

LO, C-H., CHUNG, S-L., LEE, T-Y. & WU, G. 2002, Age of the Emishan flood magnetism and relations to the Permian–Triassic boundary. *Earth and Planetary Science Letters*, **198**, 449–458.

LOZOVSKY, V. R. & MOLOSTOVSKY, E. A. 1993, Constructing the Early Triassic magnetic polarity time scale. *In*: LUCAS, S. G. & MORALES, M. (eds) *The Nonmarine Triassic*. New Mexico Museum of Natural History and Science Bulletin, **3**, 297–300.

LUCAS, S. G. 1994. The beginning of the age of dinosaurs in Wyoming. *Wyoming Geological Association, 44th Annual Field Conference, Guidebook*, 105–113.

LUCAS, S. G. & MORALES, M. 1985. Middle Triassic amphibians. *In*: LUCAS, S. G. & ZIDEK, J. (eds) *Santa Rosa-Tucumcari Region*. New Mexico Geological Society Guidebook, **36**, 56–58.

MCKEE, E. D. 1954. *Stratigraphy and history of the Moenkopi Formation near Grey Mountain*. Geological Society of America Memoir, **61**.

MENNING, M. 1986. Zur Dauer des Zechstein aus magnetostratigraphischer Sicht. *Zeitschrifte für Geologische Wissenschaften*, **14**, 395–404.

MENNING, M. 1988. Magnetostratigraphic investigation of the Rotiegendes (200–252 Ma) of Central Europe. *Zeitschrifte für Geologische Wissenschaften*, **16**, 1045–1063.

MENNING, M. 1993. A revised Permian polarity time scale. *EUG VIII Abstracts*, Strasbourg.

MENNING, M. 2000. Magnetostratigraphic results from the Middle Permian type section, Guadalupe Mountains, West Texas. *International Geological Congress, Abstracts*, **31**, pp. On CD-ROM.

MENNING M. & JIN, Y. G. 1998. Comment on EMBLETON, B. J. J., MCELHINNY, M. W., MA, X., ZHANG, Z. & LI, Z. X. Permo-Triassic magnetostratigraphy in China: the type section near Taiyuan, Shanxi Province, North China. *Geophysical Journal International*, **133**, 213–216.

MOLINA-GARZA, R. S., GEISSMAN, J. W. & VAN DER VOO, R. 1989. Paleomagnetism of the Dewey Lake Formation (Late Permian), Northwest Texas, end of the Kiaman Superchron in North America. *Journal of Geophysical Research*, **94**, 17,881–17,888.

MOLINA-GARZA, R. S., GEISSMAN, J. W., VAN DER VOO, R., LUCAS, S. G. & HAYDEN, S. N. 1991. Paleomagnetism of the Moenkopi and Chinle formations in central New Mexico: implications for the North American apparent polar wander path and Triassic magnetostratigraphy. *Journal of Geophyscial Research*, **96**, 14,239–14,262.

MOLINA-GARZA, R. S., GEISSMAN, J. W. & LUCAS, S. G. 2000. Paleomagnetism and magnetostratigraphy of uppermost Permian strata, southeast New Mexico, USA: correlation of the Permian–Triassic boundary in non-marine environments. *Geophysical Journal International*, **141**, 778–786.

MOLOSTOVSKY, E. A. 1983. *Paleomagnetic Stratigraphy of the Eastern European Part of the USSR, Saratov, Russia*. University of Saratov, Saratov. [In Russian]

MORALES, M. 1987. Terrestrial fauna and flora of the Triassic Moenkopi Formation of the southwestern United States. *Journal of the Arizona-Nevada Academy of Science*, **22**, 1–19.

MORK, A., ELVEBAKK, G., FORSBERG, A. W., HOUNSLOW, A. W., NAKREM, H. A., VIGRAN, J. O. & WEITSCHAT, W. 1999. The type section of the Vikinghogda Formation, a new Lower Triassic unit in central and eastern Svalbard. *Polar Research*, **18**, 51–82.

MUNDIL, R., LUDWIG, K. R., METCALFE, I. & RENNE, P. R. 2004, Age and timing of the Permian mass extinctions: U/Pb dating of closed-system zircons. *Science*, v. **305**(5691), 1760–1763.

MUTTONI, G., KENT, D. *et al.* 1996. Magnetobiostratigraphy of the Spathian to Anisian (Lower to Middle Triassic) Kcira section, Albania. *Geophysical Journal International*, **127**, 503–514.

NAWROCKI, J. 1997. Permian to Triassic magnetostratigraphy from the Central European Basin in Poland: implications on regional and worldwide correlations. *Earth and Planetary Science Letters*, **152**, 37–58.

NAWROCKI, J. & SZULC, J. 2000. The Middle Triassic magnetostratigraphy from the Peri-Tethys basin in Poland. *Earth and Planetary Science Letters*, **182**, 77–92.

OGG, J. G. & STEINER, M. B. 1991. Early Triassic magnetic polarity time scale, integration of magnetostratigraphy, ammonite zonation and sequence stratigraphy from stratotype sections (Canadian

Arctic Archipelago). *Earth and Planetary Science Letters*, **107**, 69–89.

ORCHARD, M. J. & KRYSTYN, L. 1998, Conodonts of the Lowermost Triassic of Spiti, and new zonation based on Neogondolella successions. *Rivista Italiana di Paleontologia e Stratigrafia*, **104**(3), 341–368.

PAULL, R. K. & PAULL, R. A. 1986, Epilogue for the Permian in the western Cordillera: A retrospective view from the Triassic. *Rocky Mountain Geology*, **24**(2), 243–252.

PAULL, R. K. & PAULL, R. A. 1990, Persistent myth about the Lower Triassic Little Medicine Member of the Goose Egg Formation and the Lower Triassic Dinwoody Formation, central Wyoming. *Wyoming Geological Association, 41st Field Conference, Guidebook*, 57–68.

PETERSON, D. N. & NAIRN, A. E. M. 1971. Paleomagnetism of Permian red beds from the southwestern United States. *Geophysical Journal of the Royal Astronomical Society*, **23**, 191–206.

PICARD, M. D., AADLAND, R. & HIGH, L. R. JR. 1969. Correlation and stratigraphy of Triassic Red Peak and Thaynes formations, western Wyoming and adjacent Idaho. *American Association of Petroleum Geologists Bulletin*, **53**, 2274–2289.

POBORSKI, S. J. 1954. Virgin Formation (Triassic) of the St. George, Utah, area. *Geological Society of America, Bulletin*, **65**, 971–1000.

PURUCKER, M. E., ELSTON, D. P. & SHOEMAKER, E. M. 1980. Early acquisition of characteristic magnetization in red beds of the Moenkopi Formation (Triassic), Grey Mountain, Arizona. *Journal of Geophysical Research*, **85**, 997–1012.

RENNE, P. R., STEINER, M. B., SHARP, W. D., LUDWIG, K. R. & FANNING, C. M. 1996. $^{40}Ar/^{39}Ar$ and U/Pb SHRIMP dating of latest Permian tephras in the Midland Basin, Texas. *Eos, Transactions of the American Geophysical Union*, **77**(46, Supplement), F794.

RENNER, J. M. 1988, *Placement and paleogeographic significance of Permian–Triassic boundary, central and Southeast Wyoming*. MSc thesis, University of Wyoming.

RENNER, J. M. & BOYD, D. W. 1988, Placement and paleogeographic significance of Permian–Triassic boundary, Southeast Wyoming. SEPM Midyear Meeting, *Abstracts*, **5**, 45.

SCHOLGER, R., MAURITSCH, H. J. & BRANDNER, R. 2000. Permian–Triassic magnetostratigraphy from the Southern Alps (Italy). *Earth and Planetary Science Letters*, **176**, 495–508.

SCHWINDT, D. M., RAMPINO, M. R., STEINER, M. & ESHET, Y. 2003. Paleomagnetic results and preliminary palynology across the Permian–Triassic (P–Tr) Boundary at Carlton Heights. *In*: KOEBERL, C. & MARTINEZ-RUIZ, F. (eds) *Impact Markers in the Stratigraphic Record*. Springer, Heidelberg, 280–302.

SMITH, R. M. H. 1995. Changing fluvial environments across the Permian–Triassic boundary in the Karoo Basin, South Africa and possible causes of tetrapod extinctions. *Palaeogeography, Palaeoclimatology, Palaeoecology*, **117**, 81–104.

STEINER, M. B. 2000, Geomagnetic polarity between the P/Tr boundary and the Kiaman termination. Eos, *Transactions of the American Geophysical Union*, **81**, F361–362.

STEINER, M. B. 2001*a*, Magnetostratigraphic correlation and dating of West Texas and New Mexico Late Permian strata. *American Association of Petroleum Geologists Bulletin*, **85**, 1695.

STEINER, M. B. 2001*b*, Magnetostratigraphic correlation and dating of west Texas and New Mexico Late Permian strata. *In*: LUCAS, S. G. & ULMER-SCHOLLE, D. (eds) *Geology of Llano Estacado*. New Mexico Geological Society, 52nd Field Conference, Guide, **52**, 59–68.

STEINER, M. B. 2004, Global magnetostratigraphic correlation of the Middle and Late Permian and the Early Triassic. *Proceedings of the 32nd International Geological Congress*, Florence, 2004, Volume 1, 746.

STEINER, M. B. & LUCAS, S. G. 1992. A Middle Triassic paleomagnetic pole for North America. *Geological Society of America, Bulletin*, **104**, 993–998.

STEINER, M. B. & RENNE, P. R. 1996. Magnetic polarity at the end of the Permian: New insights from west Texas. EOS, *Transactions of the American Geophysical Union*, **77**(46, Supplement), F164.

STEINER, M. B. & RENNE, P. 1998. Late Permian and and Permo-Triassic boundary magnetostratigraphy; progress? and problems, in Gondwana-10. *African Journal of Earth Science*, **27**(1A), 190.

STEINER, M. B., OGG, J. G., ZHANG, Z. & SUN, S. 1989. The Late Permian/Early Triassic magnetic polarity time scale and plate motions of South China. *Journal of Geophysical Research*, **94**, 7343–7363.

STEINER, M. B., MORALES, M. & SHOEMAKER, E. M. 1993. Magnetostratigraphic, biostratigraphic, and lithologic correlations in Triassic strata of the western United States. *In*: AISSAOUI, D. M., MCNEILL, D. F. & HURLEY, N. F. (eds) *Applications of Paleomagnetism to Sedimentary Geology*. Society of Economic Paleontologists and Mineralogists Special Publication, **49**, 41–57.

STEINER, M. B., ESHET, Y., RAMPINO, M. R. & SCHWINDT, D. M. 2003. Fungal abundance spike and the Permian–Triassic boundary in the Karoo Supergroup (South Africa). *Palaeogeography, Palaeoclimatology, Palaeoecology*, **194**, 405–414.

STORRS, G. W. 1991. *Anatomy and relationships of Corosaurus alcovensis (Diapsida: Sauropterygia) and the Triassic Alcova Limestone of Wyoming*. Bulletin of the Peabody Museum of Natural History, Yale University, **44**.

SZURLIES, M. 2004. Magnetostratigraphy: the key to a global correlation of the classic Germanic Trias—case study Volpriehausen Formation (Middle Buntsandstein), central Germany. *Earth and Planetary Science Letters*, **227**, 395–410.

SZURLIES, M. B., GERHARD, H., MENNING, M., NOWACZYK, N. R. & KAEDING, K. C. 2003. Magnetostratigraphy and high-resolution lithostratigraphy of the Permian–Triassic boundary interval in central Germany. *Earth and Planetary Science Letters*, **212**, 263–278.

SWEET, W. C. & BERGSTROEM, S. M. 1986. Conodonts and biostratigraphic correlation. *Annual Reviews of Earth and Planetary Sciences*, **14**, 85–112.

THOMAS, H. D. 1934, Phosphoria and Dinwoody tongues in lower Chugwater of central and southern Wyoming. *American Association of Petroleum Geologists Bulletin*, **18**, 1655–1697.

TOZER, E. T. 1967. A Standard for Triassic Time. *Geological Survey of Canada, Bulletin*, **156**.

VALENCIO, D. A., VILAS, J. F. A. & MENDIA, J. E. 1977. Paleomagnetism of a sequence of red beds of the middle and upper sections of Pagnazo Group (Argentina) and the correlation of Upper Paleozoic-Lower Mesozoic rocks. *Geophysical Journal of the Royal Astronomical Society*, **51**, 59–74.

WARD, P. D., BOTHA, J. *et al.* 2005. Abrupt and gradual extinction among Late Permian land vertebrates in the Karoo Basin, South Africa. *Science*, **307**, 709–714.

WARDLAW, B. R. 2003. Global Guadalupian (Middle Permian) conodont correlation and distribution. *Permophiles*, **42**, 20–21.

WARDLAW, B. R. & COLLINSON, J. W. 1986. Paleontology and deposition of the Phosphoria Formation. *Rocky Mountain Geology*, **24**, 107–142.

WARDLAW, B. R. & POGUE, K. R. 1995. The Permian of Pakistan. *In*: SCHOLLE, P. A., PERYT, T. M. & ULMER-SCHOLLE, D. S. (eds) *The Permian of northern Pangaea, Vol. 2.* Springer-Verlag, Berlin, 215–224.

WESTPHAL, M., GUREVICH, E. L., SAMSONOV, B. V., FEINBERG, H. & POZZI, J-P. 1998. Magnetostratigraphy of the Lower Triassic volcanics from deep drill SG6 in western Siberia, evidence for long-lasting Permo-Triassic volcanic activity. *Geophysical Journal International*, **134**, 254–266.

ZAKHAROV, Y. D. & SOKAREV, A. N. 1991. Permian–Triassic paleomagnetism of Eurasia, *In*: KOTAKA, T., DICKENS, J. M., MCKENZIE, K. G., MORI, K., OGASAWARA, K. & STANLEY, G. D. JR. (eds) *Proceedings of the International Symposium on Shallow Tethys*, **3**, 313–323.

ZEISSL, W. & MAURITSCH, H. 1991. The Permian-Triassic of the Gartnerkofel-1 core (Carnic Alps, Austria), Magnetostratigraphy. *Abhandlungen der Geologischen Bundesanstalt*, **45**, 193–207.

ZHU, Y-M. & LIU, Y-Y. 1999. Magnetostratigraphy at the Permian–Triassic boundary at Meishan, Changxing, Zhejiang Province. *In*: YIN, H. & TONG, J-N. (eds) *Proceedings of the International Conference on Pangaea and the Paleozoic-Mesozoic Transition China University of Geosciences, Wuhan, September 1999*. Geoscience Press, 79–84.

ZIU, Y., ZHU, Y. & TIAN, W. 1999. New magnetostratigraphic results from Meishan section, Changxing County, Zhejiang Province. *Earth Science, Journal of China University of Geosciences*, **24**(2), 151–154.